Nanocontact printing on soft substrates: haptotaxis on netrin-1 digital nanodot gradients

Donald MacNearney

donald.macnearney@mail.mcgill.ca

Department of Biomedical Engineering

McGill University, Montreal

A thesis submitted to

McGill University

in partial fulfilment of the requirements of the degree of

Master of Engineering

in Biomedical Engineering

June 2016

Department of Biomedical Engineering

Room 316, Duff Medical Building

3774, rue University

Montreal, QC, H3A 2B4

CANADA

Abstract

Cellular navigation, migration, and motility are vital requirements for life, whether it be during the development of an organism, or throughout the life cycle – for example during tissue maintenance and wound healing. This process is regulated by continuous integration of multiple extracellular cues. Surface bound chemical cues regulate cell navigation in many cells including neutrophils, myoblasts, and developing neurons through a process known as haptotaxis. Mechanical cues, in the form of substrate stiffness, can also regulate cell motility, for example through a process known as durotaxis. Based on these observations, alterations in substrate stiffness may have an impact on guided cellular migration via haptotaxis. Haptotaxis has been demonstrated on digital nanodot gradients (DNGs) of protein guidance cues, but to date these experiments have only been performed on hard surfaces. At present there is no existing technique to create protein patterns with nanometer scale features on soft and tacky substrates. Here we present a novel technique for patterning digital nanodot gradients (DNGs) on soft substrates (E $<$ 10 kPa). DNGs of netrin-1 (a known axon guidance cue) were patterned on Sylgard 527, a very low modulus poly(dimethylsiloxane) (PDMS). The un-patterned surface was backfilled with a reference surface of 75% poly-ethylene glycol grafted with poly-lysine and 25% poly-D-lysine, to tune the reference cell-surface affinity and enhance the cell sensitivity to the patterned gradient. C2C12 myoblasts were cultured on the patterned substrates, and cell positions were recorded over time. Cell distributions were observed to significantly shift towards higher density areas of netrin-1 over a time period of 18 h, signifying a haptotactic response to the patterned gradients on soft substrates. Live imaging of cells on sinusoidal gradients highlighted cells migrating and navigating by 'inching'. This work represents the first time that protein patterns with feature sizes in the nanometer range have been successfully patterned via lift-off nanocontact printing on substrates with stiffnesses $<$ 10 kPa. As well, this is the first study which demonstrates a haptotaxis migration assay on a soft substrate. This experimental technique may be used in future projects to study haptotaxis on surfaces of varying rigidities, providing additional insight into how cells integrate multiple environmental signals to make navigational choices.

Résumé

La navigation, la motilité et la migration cellulaire sont requis pour la vie, que ce soit pendant le développent de l'organisme, ou au travers du cycle de vie – par exemple pendant la réparation du tissue et la cicatrisation. Ce processus est régulé en assimilant continuellement plusieurs signaux extracellulaire. La navigation cellulaire de plusieurs types de cellules tel les neutrophiles, les myoblastes et les neurones en développement est régulée par l'haptotaxie ou les chimioattractants et les chimiorepellants se presentent sur les surfaces. Les signaux mécaniques, comme la rigidité du substrat, peuvent aussi régulé la motilité cellulaire par durotaxie. Il est donc possible que la rigidité du substrat ait un impacte sur la migration cellulaire guidé par haptotaxie. Le processus de haptotaxie a été démontré sur des 'digital nanodot gradients' (DNGs) de protéines chimioattractantes, mais ces manipulations ont seulement été faites sur des surfaces dures. Il n'y a pas de méthode existante pour produire des motifs de protéines à l'échelle nanométrique sur des substrats mous et collants. Nous présentons une nouvelle technique pour créer des DNGs sur des surfaces molles ($E < 10$kPa). DNGs de netrin-1 (un signal de guidage des axones connu) ont été crée sur du Sylgard 527, un poly(diméthylsiloxane) (PDMS) avec un coefficient d'élasticité très petit. La surface sans motif a été remplie avec une surface référence de 75% glycol polyéthylénique greffé avec de la polylysine et 25% de poly-D-lysine, pour contrôler l'affinité des cellules pour la surface de référence et améliorer la sensibilité de la cellule au gradient sur la surface. Les myoblastes C2C12 ont été mis en culture sur les substrats avec les motifs et la position des cellules a été mesurée dans le temps. La distribution des cellules a été déplacée de façon significative vers la plus haute concentration de netrin-1 sur 18 h, signifiant une rṕonse haptotactique au gradient imprimé sur le substrat mou. Imagerie en temps réel des cellules sur des gradients sinusoïdales a souligné les cellules qui migrent et naviguant au 'inching'. Ce travail est la première fois que des motifs de protéines a l'échelle nanométrique a été imprimé par un processus de 'lift-off nanocontact printing' sur des substrats avec une rigidité < 10 kPa. C'est aussi la première étude qui démontre l'haptotaxie sur un substrat mou. Cette technique expérimentale pourra être utilisée pour l'étude de l'haptotaxie sur des surfaces

avec différentes rigidités, fournissant un nouvel aperçu sur comment les cellules assimilent plusieurs signaux environnementaux pour décider leur navigation.

Acknowledgements

First and foremost, I would like to thank Prof. David Juncker for agreeing to supervise me throughout my degree, and providing me with the lab space and resources that made this work possible. My colleagues at the lab were of great help during my stay at McGill - in particular Sébastien Ricoult and Abhishek Sinha were very helpful and provided invaluable discussions when it came to the details of my project, and Bernard Mak was a great help during the summer he worked as an undergraduate researcher under my supervision. Furthermore, I wish to thank Ayokunle Olanrewaju, Phillipe Decorwin-Martin, and Fred Normandeau for their friendship and attentive ears when I needed them. All other members of the lab were also extremely helpful - I feel lucky to have had such a great group of people to work with. On a personal note, I would like to thank Chloé Baruffa for her support during some hard months, and Natasha Larrivé for her unwavering friendship. Finally, I wish to thank my family for continuing to be there for me whenever I needed it most.

Donald MacNearney received funding from an NSERC CGSM award, from the NSERC CREATE Neuroengineering program at McGill, and from the NSERC CREATE Integrated Sensor Systems program at McGill.

Contents

List of Figures

1 Project Description

1.1 Motivation

The motivation for this work is to develop a better understanding of cellular navigation, and in particular to understand how the stiffness of the cellular microenvironment can impact cellular navigation. Previously, a technique for patterning surface bound gradients of proteins was developed [1], which was used for performing haptotaxis assays. This technique allows for rapid, repeatable, and cost-effective patterning of large areas with surface bound gradients composed of digital nanodots, and provides an excellent way to isolate the process of haptotaxis in an experimental setting. While the technique was initially developed with the intention of investigating axon turning events on netrin-1 gradients, it was demonstrated that surface bound gradients of netrin-1 can also attract C2C12 cells, due to their expression of Neogenin, a receptor for netrin-1. This makes C2C12 cells on netrin-1 gradients a useful model system to validate the functionality of surface bound gradients. The intention is to use these types of gradients to investigate axon turning in the future, and this is reflected in our choice of printed guidance protein – the axon guidance cue netrin-1.

Numerous observations have been made in the literature that the mechanical properties of the extracellular environment can influence cell behaviour. Specifically, the elastic modulus of the substrate material can alter cell adhesion and motility [2], and axons extend more rapidly [3] and more extensively [4] on softer substrates, with stiffnesses that are more representative of the *in vivo* microenvironment. In lieu of this information, we wanted to investigate whether lowering the substrate stiffness to these levels would affect the haptotactic response of a cell when presented with a gradient of surface bound cues. To our knowledge, the investigation of haptotaxis on substrates with a very low elastic modulus has not been done before.

Our choice of soft substrate is also related to our long term goal to apply this concept

to axon turning in the future. To this end, this work used the material Sylgard 527, which has an elastic modulus close to that of brain tissue (< 10 kPa [5]), and which has previously been used as a soft substrate for cell culture [6–9].

1.2 Project Goals

There were two main goals for this project, which were to (i) adapt the technique of lift-off nanocontact printing to soft substrates and demonstrate that the process allows for patterning of digital nanodot gradients (DNGs) on Sylgard 527, and (ii) demonstrate the functionality of these gradients by performing a haptotaxis assay on netrin-1 gradients patterned on Sylgard 527.

1.3 Manuscript-based Thesis

This thesis will be presented in manuscript form – an introduction section will provide the necessary background information, followed by the body of the work, presented as a pre-print manuscript, with the intention that this will be submitted for peer review and publishing in the near future. Finally, discussion and conclusion sections will provide more general discussion of the results and suggestions for future work that are not included in the manuscript.

1.3.1 Contribution of Authors

For the manuscript, Donald MacNearney performed almost all experiments and all of the data analysis, figure preparation, and writing. Bernard Mak helped to develop the technique for printing on Sylgard 527, and captured the image in Figure 3.2(d) during these early experiments. Prof. Kennedy provided his expertise in the field to help review and edit the manuscript, as well as providing the netrin-1 protein from his lab, which was used in the experiments. Prof. Juncker supervised the project and offered his guidance throughout the process. This thesis was prepared by Donald MacNearney, with revision help from Prof.

Juncker.

1.4 Declaration of Novelty

To the best of our knowledge, this work represents the first time that protein patterns with feature sizes in the nanometer range have been successfully patterned via lift-off nanocontact printing on soft, tacky substrates with stiffnesses < 10 kPa. As well, this is the first study which demonstrates a haptotaxis migration assay on soft substrates.

2 Introduction

In vivo cellular migration is essential for life, and may be seen as a stochastic or random process with directional biases imposed by guidance factors in the environment [10]. From yeast and bacterial migration towards food sources to wound healing and organogenesis in complex multicellular organisms, the ability to continuously integrate and respond to environmental stimuli is ubiquitous in biological systems. Cells respond to a variety of stimuli, such as chemical guidance cues, mechanical stresses, and topography, to name a few [11]. Here the mechanisms of guided cellular motility relevant to this work will be reviewed, giving the necessary background to contextualize the work presented in this thesis. In particular, the focus will be on two modalities of directed cell migration - migration via biochemical guidance cues, and migration due to mechanical influences from the cellular microenvironment. The introduction is thus organised as follows: the first two subsections introduce (i) guided cellular navigation via biochemical gradients, with a focus on surface bound gradients, and (ii) current techniques to recreate these gradients *in vitro*; the next two subsections describe (iii) how altering the mechanical properties of the extracellular environment can alter cell behaviour, and (iv) current techniques used to investigate this phenomenon; the final subsection (v) discusses current efforts to incorporate different mechanical properties into biochemical assays to investigate the interplay of these two modalities.

2.1 Cellular Navigation by Biochemical Gradients

Many cellular processes are mediated by a series of complex *in vivo* gradients, both soluble and surface bound. Cellular migration and differentiation due to chemical gradients play key roles during organism development, for example during neural crest migration and brain development [12,13], limb patterning [14], and cell differentiation during drosophila development [15]. These gradients are essential for life as we know it, and as such the understanding of these gradients and how cells respond to them is crucial for developing a more complete picture of how the human body develops.

Two main types of chemical gradients found *in vivo* are surface bound gradients and soluble gradients. Soluble gradients may be formed by secreted proteins from a group of cells, forming a source that can develop into a gradient via free diffusion, while endocytosis of these proteins may take the role of a sink, thereby preventing saturation of the extracellular space with signalling molecules [16,17]. Surface bound gradients may arise as a result of these diffusible molecules becoming bound to the extracellular matrix, or by spatial variation of membrane bound protein expression between groups of cells [18,19].

The mechanisms by which cells respond to surface bound gradients and soluble gradients are termed haptotaxis and chemotaxis, respectively. While these two terms describe similar processes – namely, the directional motility of a cell in response to a chemical gradient – it has been postulated for quite some time that these processes are mediated by different cellular mechanisms [20].

Chemotaxis vs. Haptotaxis Chemotaxis has been widely studied in a large variety of biological systems. Briefly, the term chemotaxis refers to directed cell motility up a concentration gradient of soluble extracellular signalling molecules. Chemotaxis is crucial in many biological functions, such as in embryological development and organization, finding food

sources in prokaryotes, and combatting bacterial infections by neutrophils [21]. Depending on the cell type and size, chemotactic movement may be mediated by different mechanisms. In smaller cells (i.e. prokaryotes), it is not possible for an individual cell to sense the concentration gradient directly, and the cells move with a biased random walk, whereby an increase in chemoattractant will extend movement in a given direction, leading to collective movement towards the source over time [21,22]. In larger cells (i.e. eukaryotes), it is possible to directly sense the concentration gradient of an attractant as a difference in concentration across the cell body. Surface receptors in the cell respond to chemical cues and transduce this signal into a polarized reorganization of the cytoskeleton, eventually leading to directed movement towards the source of the cue [23].

The term haptotaxis was coined in 1965 [24]. In comparison to chemotaxis, haptotaxis has been relatively unstudied. At the time of writing this, only 245 papers on PubMed are returned with a search for 'haptotaxis'. Despite this relative obscurity, it has been postulated for many years that haptotactic motility represents a distinct mechanism from chemotaxis - for example, inhibiting chemotactic responses yields no observable changes in haptotactic responses in the same experiments [25], and morphological differences have been observed between cells undergoing chemotaxis and haptotaxis [26]. However, because both chemotaxis and haptotaxis are forms of directed cell migration in response to chemical gradients, there is still an ongoing debate over the true nature of the difference between these two processes [27]. Despite this debate, in this text I will be referring to directed cellular motility responses to soluble cues as chemotaxis, and responses to substrate bound cues as haptotaxis.

2.1.1 Haptotaxis in Neuroscience

Chemical guidance is a central feature of the development of the nervous system, and numerous axon guidance molecules have been identified, including robo and slit proteins, ephrins, semaphorins, and netrins [28–32]. While chemotaxis in the nervous system has been widely documented, there are examples of haptotactic mechanisms at play as well, particularly in

growth cone migration during development. Initially it was shown that growth cones of retinal ganglion cells would respond to smooth gradients of surface bound proteins – in these early examples, the gradients were made with fragmented cell membranes from tectal cells. It was found that the cell membranes from the posterior optic tectum possessed a repulsive guidance protein, and that temporal retinal ganglion axons preferred to grow on anterior tectal cell membranes, which did not express this protein [33, 34]. It was shown later that a family of membrane proteins named ephrins mediate the development of the retinotopic map through axon repulsion [35]. Another family of axon guidance cues known as netrins have also been implicated as a substrate bound cue, in addition to their previously studied role as long-range diffusive chemical guidance molecules [36]. Local expression of netrin-1 on retinal cell membranes has been shown to allow retinal ganglion cell axons to exit the eye and enter the optic nerve [37]. Tethered netrins have also been implicated in the facilitation of commisural axons crossing the midline in Drosophila embryos, a process which appears independent of the guidance of axons towards the membrane by diffusive Netrin [38]. There is a growing body of evidence that suggests that netrins play an important role in the developing nervous system as a short range, substrate bound guidance cue [36], and as a result the development of substrate bound protein gradients to study the process of haptotaxis has been of increasing interest [27].

Netrin-1: Function and Structure Netrin-1 is part of a family of secreted proteins, consisting of approximately 600 amino acids, with a molecular weight of 75 kDa [39–41]. Other members of the family are netrin-3 and netrin-4. The netrin-1 protein consists of an N-terminal domain (VI), three repeated domains (V-1, V-2, and V-3), and a C-terminal domain which is positively charged [42]. Its main receptors in the nervous system are Deleted in Colorectal Carcinoma (DCC), UNC5H, and Neogenin [43, 44]. Of these receptors, Neogenin is also expressed in cell types present outside of the nervous system, for example in C2C12 myoblast cells [45] and in cap cells of terminal end buds in the mammary gland [46]. Based on these studies, netrin-1 has been postulated to be a key biochemical signalling molecule in non-neuronal systems as well. In this work the C2C12 myoblast cell line was used, because

these cells are robust and easy to work with, and also express Neogenin and respond to netrin-1.

2.2 Biochemical Gradient Generation *in vitro*

Because of the ubiquitous nature of biochemical gradients *in vivo*, a key area of research for many years has been attempting to recapitulate these gradients *in vitro*, to better study and understand their roles in biological processes. The two types of chemical gradients described above – solution based and surface bound gradients – have both been investigated, due to the ongoing belief that these two types of gradients act through different mechanisms. As the focus of this work is on haptotaxis and surface bound gradients of proteins, techniques for creating surface bound gradients *in vitro* will be discussed here. First, however, when speaking of surface bound gradients, it is important to discuss the chemical composition of the un-patterned surface, denoted the reference surface, as this surface will impact the cellular response.

2.2.1 Reference Surfaces in Surface Bound Gradients

An important consideration in the creation of surface bound gradients is the presence of an opposing gradient, denoted the reference surface gradient, which consists of the un-patterned areas of the substrate in the same area as the patterned gradient (Figure 2.1) [27]. In all cases, the presence of the reference surface gradient affects the cellular response to the patterned gradient; if no reference surface is specifically applied, then it takes the form of the underlying substrate. As cells display different degrees of adhesion to different substrates, the reference surface can impact the outcome of experiments if it is not controlled for. A technique for controlling the chemical composition of the underlying reference surface is to backfill the substrate with a chemically defined solution, and allowing that solution to coat the surface in any place where the patterned proteins are absent.

It should be noted that the presence of a reference surface is one way in which a surface bound gradient is conceptually different from a soluble gradient, as the concept of an opposing surface bound gradient has no meaning when related to gradients in solution. It is also of interest to note that the relative change of the reference surface related to the relative change of the patterned gradient is different at different areas of the gradient. For instance, at the low end of the patterned gradient, if the density of patterned protein changes from 1% to 2% of the surface area, while the reference surface density changes from 99% to 98% of the surface area, the change in the density of the patterned protein is relatively much higher than the change in the reference surface density. Near the higher end of the gradient, the opposite is true. Thus, conceptually, the reference surface takes on the greatest importance near the higher end of the patterned gradient.

Previous work demonstrating the application of controlled reference surface gradients used polymers with high (i.e. polylysine) and low (i.e. poly(ethylene glycol)) affinity for cellular adhesion, and mixed these at different ratios to tune the overall affinity of the reference surface coating on the substrate [47]. By tuning the affinity of the reference surface, the cellular response to the patterned gradient may be altered. For example, a very low affinity reference surface can force a migration response even to a very weak or non-specific adhesive cue, while a very high affinity reference surface can mask a response to a guidance cue. The reference surface has been proposed as a way to quantify the strength of a migratory response to a guidance cue - chemical cues which elicit a response even on high affinity reference surfaces can be said to exert a stronger response than a cue which only elicits a response on a lower affinity reference surface [27].

2.2.2 Generating Surface Bound Protein Gradients

The first protein gradients patterned on surfaces for *in vitro* studies were demonstrated in the 1980s [48]. In this work, the gradients took the form of an abrupt change between two

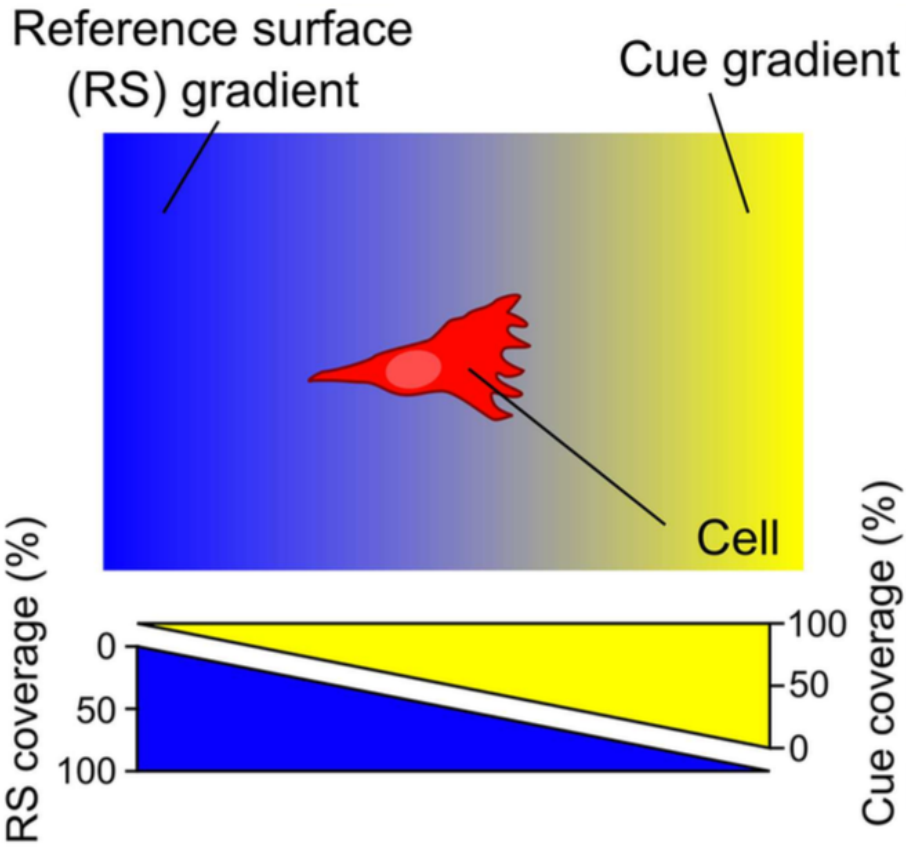

Figure 2.1: The opposing reference surface gradient present in surface bound protein gradients. As the reference surface consists of the un-patterned surface, the density profile for the reference surface gradient is effectively just the inverse of the density profile for the patterned cue. Adapted from [27].

types of proteins, as alternating stripes of the different proteins were patterned on a membrane. A silicon matrix with a stripe pattern (Figure 2.2(a)) was placed on a membrane and a solution of dissociated cell membranes was flowed through the channels, patterning the substrate. The matrix was then removed and a second solution of protein was added, patterning the area protected by the silicon in the first step. This assay is still used today in neuroscience studies, and is commonly denoted the stripe assay [49]. Two recent examples of this technique being applied to study axon guidance involve measuring the number of axons in an outgrowth assay that grow on each type of stripe [50], or measuring the rate of actin retrograde flow in individual growth cones on different stripes [51]. Putting these stripes into a biological context, abrupt changes in protein distributions exist *in vivo* as well; for

example the transition from nasal to temporal protein expression patterns in the retina is very abrupt [48]. In general these assays are useful for measuring cell preferences between substrate bound cues, as an early form of migration assay.

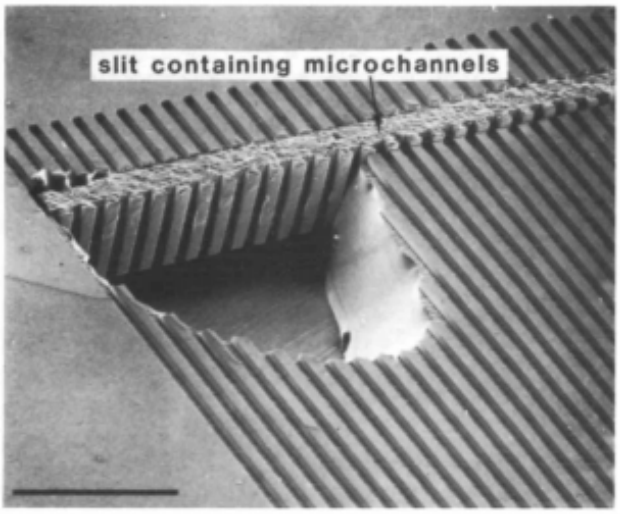

(a) Silicon matrix used to create surface bound stripes of protein. Adapted from [48]

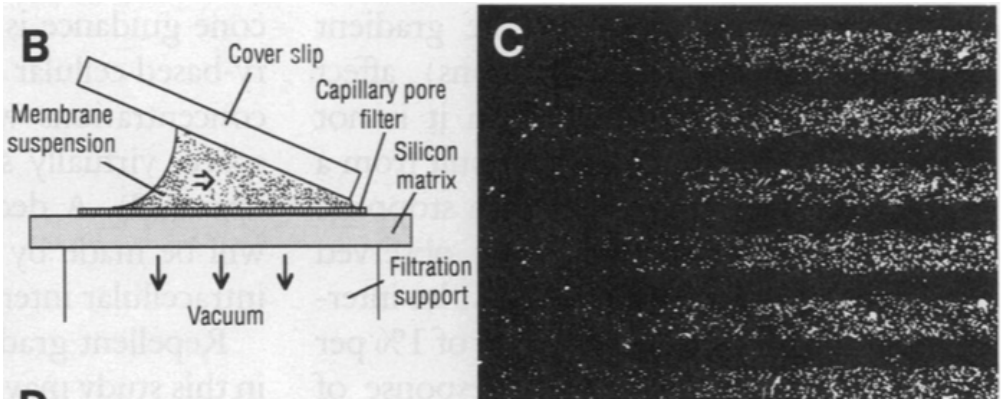

(b) Stripe gradients created using a modification of the stripe assay. A coverslip is held at an angle above the silicon matrix, such that a concentration gradient of protein is created along the stripes. Adapted from [33].

Figure 2.2: Early generation of substrate bound gradients

Continuous gradients of surface bound proteins may be generated using a modification of the technique for creating a stripe assay. A gradient is created along the length of the stripes by asymmetrically spreading the protein solution across the silicon stripe pattern using a coverslip, which is held over a drop of protein solution with one edge raised (Figure 2.2(b)) [33].

Microfluidic channels may also be used to generate surface bound gradients, as the proteins will adsorb to the underlying substrate over time. The microfluidic device may then be removed, leaving behind the protein gradient on the substrate (Figure 2.3(a)) [52–54]. Microfluidic probes may also be used to adsorb protein patterns to surfaces by flowing a stream of protein solution over a confined area of a surface, and moving the probe laterally at varying speeds (Figure 2.3(b)) [55].

Other techniques include diffusing solutions of protein through hydrogels, leading to adsorption of the proteins on an epoxy-coated glass substrate and formation of a substrate bound gradient [56], or by using laser-induced photobleaching to selectively initiate binding of proteins to a surface in a reaction utilizing the free radicals released in the photobleaching [57, 58]. However, with all of these methods it is difficult to accurately control and characterize the resulting gradients, as fluorescence imaging has inherent quantification difficulties caused by background flourescence and photobleaching. Quantifiable gradients have been made by patterning digital gradients, instead of continuous gradients. Digital spots of protein are patterned, and by changing the size and spacing of spots, it is possible to calculate the surface density of the patterned gradients based on the design parameters [59–61]. Additionally, there is evidence that the spacing between protein anchors on a surface can affect cell activity [62]. Patterning digital protein spots with variable spacings may be used to investigate this phenomenon, in addition to providing advantages in quantification. The most common technique for patterning these digital spots of proteins is microcontact printing.

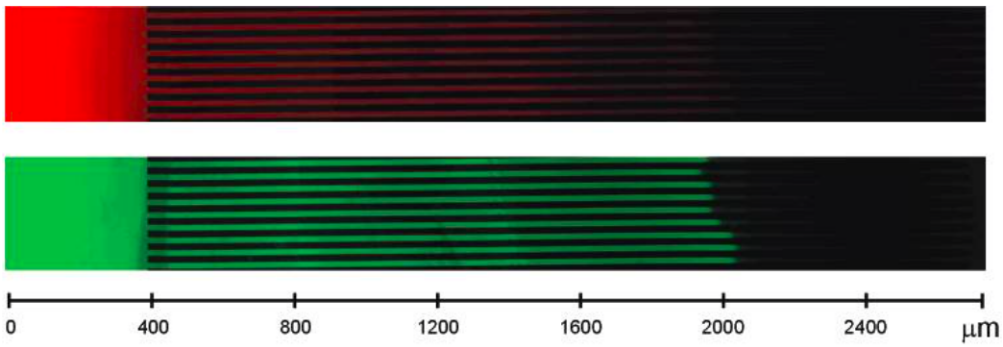

(a) Surface bound gradients made using microfluidic channels. Adapted from [53]

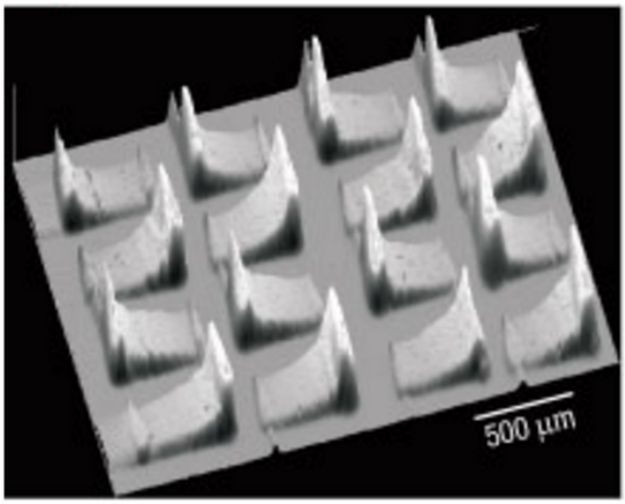

(b) Surface density gradients made with the microfluidic probe. Adapted from [55]

Figure 2.3: Early generation of substrate bound gradients

Microcontact Printing Microcontact printing was originally reported in 1994 by the Whitesides group at Harvard [63]. At the time it was presented as a microfabrication technique available outside of the clean room, and not as a technique for protein patterning (this application evolved later). In the original work, alkanethiols were incubated in an ethanol solution on top of PDMS stamps, and, as cured PDMS remains permeable to small molecules, the solution diffused into the polymer network of the PDMS over time. When the excess solution was washed away and the stamp dried, some ethanol with thiols remained inside

the stamp, and would diffuse out when the stamp was then inverted and pressed onto a substrate. The substrates used were coinage metals, such as copper and gold, because it was known that alkanethiols would self-assemble into monolayers on these surfaces [64, 65]. The end result was a monolayer of alkanethiols on the gold surface, in the shape of the stamp pattern. This was then used as an etch stop for wet-etching into the gold layer, thus completing the cycle – achieving microfabrication without the need for a microfabrication facility.

In general, microcontact printing is a fairly simple and robust patterning technique that allows repeatable and low cost replication of one dimensional patterns on flat surfaces [66,67]. It is analogous to stamping ink patterns on paper. Essentially, the desired pattern is generated on a disposable stamp, coated with an 'ink', and then inverted and pressed onto a substrate, leaving behind the inked pattern only where the raised features were present on the stamp [68, 69]. The inking solution may take a variety of forms – examples of inking solutions include alkanethiols in ethanol solution [70], proteins [59, 66], bacterial cells [71], and quantum dots [72]. Following an incubation period, the length of which depends largely on the type of ink being used, the excess ink is washed away and the stamp is dried briefly before being inverted and contacted with the final substrate. While in contact, the ink will transfer from the raised features of the stamp to the final substrate, replicating the pattern and completing the process. A notable distinction should be made in the case of protein patterning: the protein 'ink' is said to be a dry ink, as the excess liquid is dried before printing and the transfer between substrates occurs in a dry state. This is different from common printing with viscous inks, as well as the original demonstration of microcontact printing of thiols in ethanol solution, as the ink in each of these examples is in solution.

Microcontact printing of micron scale features and patterns onto surfaces has evolved to address numerous applications. By altering the inking solution, the pattern on the stamp, and the final substrate to be printed on, a wide range of possibilities exist. Some alternative inking solutions have already been mentioned above, however in recent years the most common application of micro-contact printing has been to pattern proteins in repeatable and

controlled patterns to facilitate *in vitro* biological assays. A recent example of the applications of microcontact printing of proteins may be seen in [73], and a generalized diagram of microcontact printing of proteins may be seen in Figure 2.4.

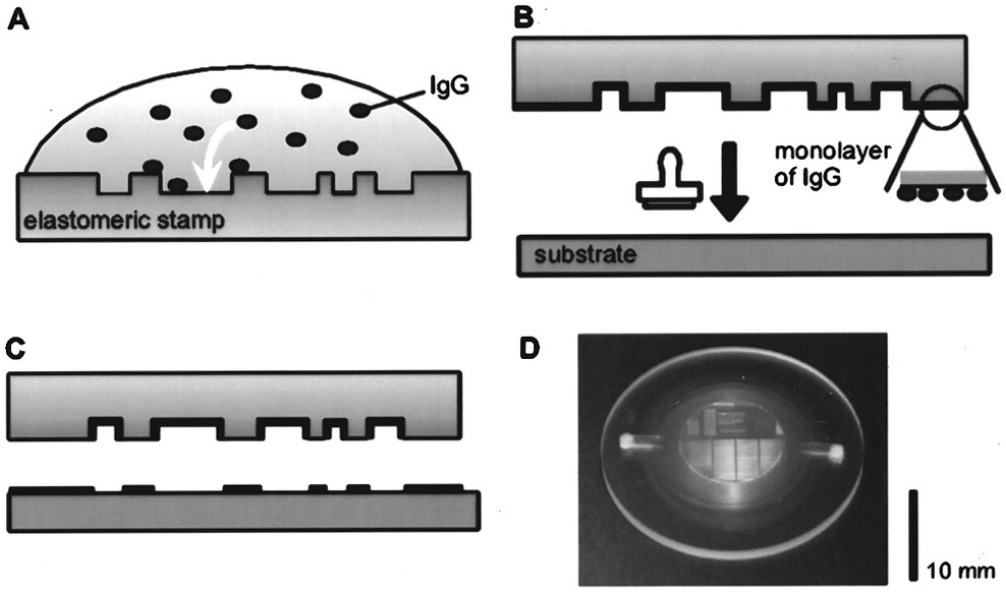

Figure 2.4: Microcontact printing of proteins: inking and printing. Protein solution is first incubated on an elastomeric stamp. Once a layer of protein has adsorbed, the remaining solution is rinsed away and the stamp is dried before being inverted and pressed onto the substrate. The raised features of the stamp determine where protein is transferred to the substrate. Finally, a patterned wafer is shown, as an example of a mold used to fabricate the elastomeric stamps. Adapted from [66].

Lift-off Microcontact Printing One major limitation of microcontact printing is that the size of printable features is limited by the deformable nature of the elastomeric stamp. Lateral collapse and sagging can obfuscate the desired pattern if the features are too small or too far apart [68, 74]. This limitation may be overcome to a large degree by employing a double replication step in the printing process (Figure 2.5) [59, 75]. Essentially, a negative of the desired pattern is created through a double replication process. The desired protein solution is incubated on a flat stamp of PDMS in this case, rather than on a stamp with raised features. The flat stamp is brought into contact with the negative mold, and all undesired

protein is stuck to this negative. Then the flat stamp is contacted with the final substrate, at which point the desired pattern is deposited. The negative mold used for lifting off undesired protein may be made from a material much stiffer substrate than PDMS, thus effectively eliminating lateral collapse, though sagging of the PDMS stamp onto the negative mold may still be an issue. However, this technique is typically used to generate very small features, thereby avoiding sagging during the lift-off step. The contact between the stamp and the final substrate is made by two flat surfaces, so no collapse is possible, allowing for a much wider range of possible feature sizes and aspect ratios than with conventional microcontact printing alone.

To properly understand how proteins can transfer between surfaces so effectively in microcontact printing, it is important to have some understanding of the molecular interactions at work. Microcontact printing works by adsorption of proteins onto surfaces with successively higher surface energies. Protein adsorption to a surface depends on the strength of the non-covalent interactions present at that interface. These interactions include hydrogen bonds, hydrophobic and electrostatic interactions, and van der Waals forces [76, 77]. To ensure high quality protein transfer during microcontact printing, it is typical to activate the final substrate (usually a glass slide) with oxygen or compressed air plasma, which adds -OH bonds to the surface of the substrate and raises its surface energy. When the stamp is initially inked with protein solution, proteins will adsorb to the surface of the PDMS stamp, though the forces holding them there will be relatively weak when compared to the forces pulling the proteins to the plasma activated glass – thus, plasma activation of the glass substrate facilitates protein transfer.

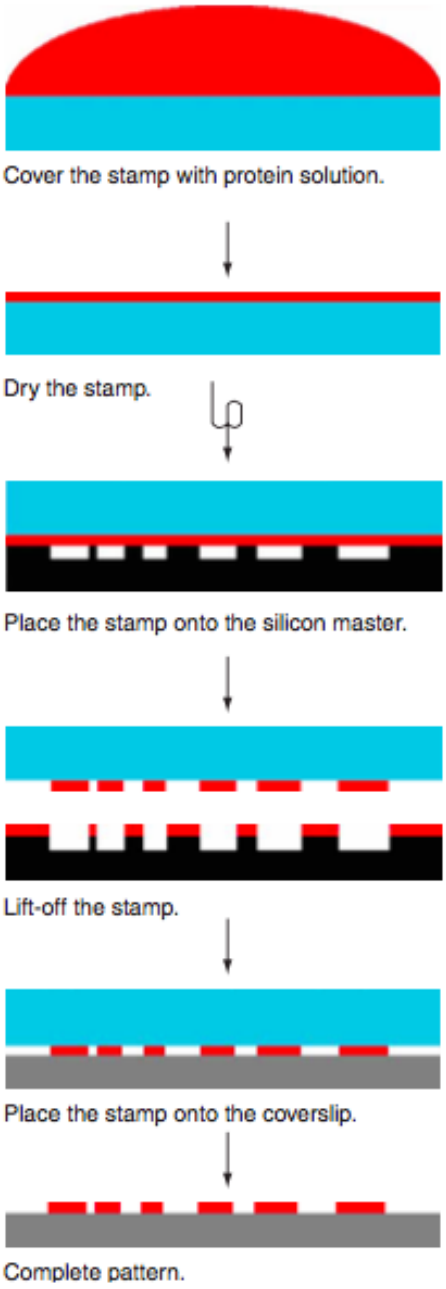

Figure 2.5: Lift-off microcontact printing. While similar to standard microcontact printing, this technique uses an additional lift-off step to replicate the protein pattern on a flat elastomeric stamp, rather than on a stamp with raised features. This eliminates the concerns of collapse and allows for patterning of sub-micron features. Adapted from [59].

Humidified Microcontact Printing In certain cases, it may be desirable to pattern proteins on surfaces that are not plasma activated, do not have high surface energy, or otherwise do not form strong non-covalent interactions with proteins. In these cases, the techniques described above cannot be applied, because the protein transfer will not be facilitated by the increased surface energy of the final substrate, and protein transfer will not occur. To overcome this limitation, a variant of micro-contact printing was developed, called humidified micro-contact printing (HμCP), which utilises the permeability of PDMS to pass water vapour and desorb proteins on the surface of a plasma activated PDMS stamp (Figure 2.6) [78].

While the molecular interactions causing this transfer to occur are not completely understood, modelling has presented the following theory: water molecules present at the interface of a protein and a surface will interact with the surface, forcing the presence of a thin layer of water between the protein and the surface, and ultimately desorbing the protein. This process is facilitated if the surface is hydrophilic, and in humidified microcontact printing the stamp is plasma activated, introducing -OH bonds to the surface and increasing its hydrophilicity. As the final substrate is not plasma activated and is therefore less hydrophilic (when speaking of glass and PDMS substrates, plasma activation is generally synonymous with increased hydrophilicity), the desorbed proteins will adsorb to this substrate through a series of hydrophobic interactions.

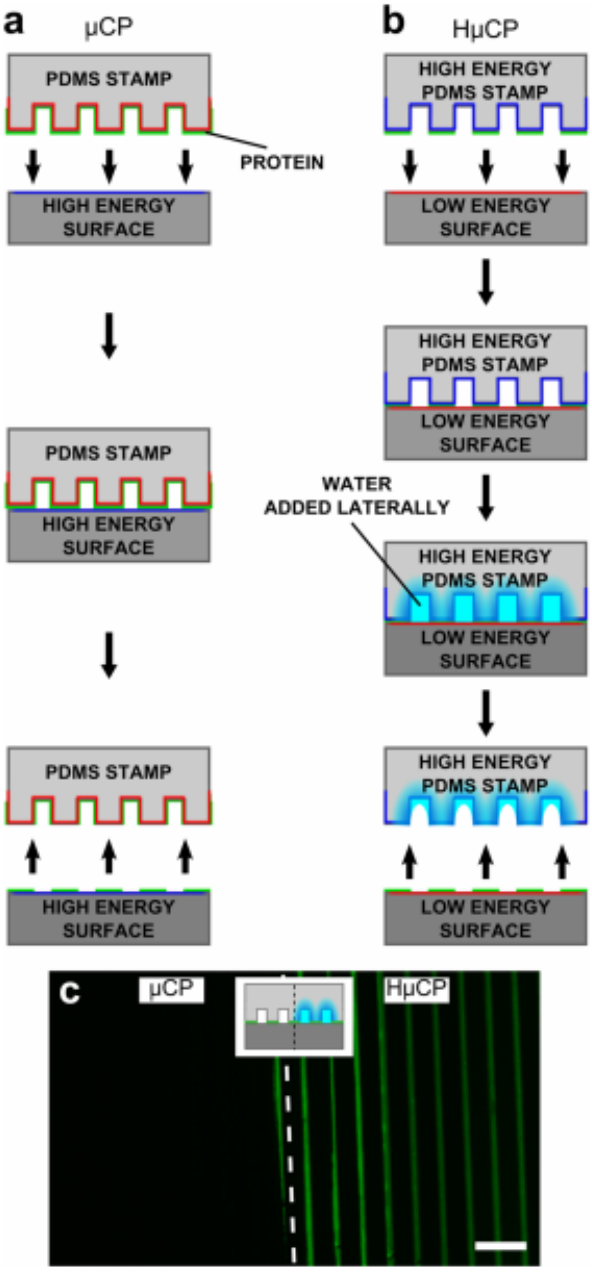

Figure 2.6: Humidified micro-contact printing. This technique uses the presence of water molecules to desorb proteins from high surface energy stamps and allow them adsorb to a low surface energy substrate. When using HμCP, protein transfer occurs from a high energy surface to a low energy surface, but not between two high energy surfaces, due to the interactions between water molecules and high energy surfaces blocking protein adsorption. Adapted from [78].

Techniques for Nanopatterning of Proteins Using lift-off microcontact printing, the limitations associated with collapse of elastomeric stamp patterns can be largely eliminated. This allows for patterning sub-micron features, and when speaking of patterning digital gradients of surface bound protein spots, the ability to pattern nanometer size spots increases the potential precision and dynamic range of the patterned gradients. In the originally reported lift-off technique, a silicon wafer was patterned with very precise nanometer features using electron beam lithography [75]. This wafer could be used as a nano-template to remove protein from the surface of an elastomeric stamp, leaving behind only the desired proteins in nanometer scale spots. However, over time the surface of this wafer can degrade, due to the continued recycling of protein coats on its surface. A low cost version of this technique, dubbed low-cost nanocontact printing, uses a double replication step to replicate the silicon master mold features on a disposable template. By first replicating the master into PDMS, before the second replication of the pattern into a UV curable polyurethane, this process extends the life span of the silicon wafer, reducing the cost per print (Figure 2.7) [1]. This technique was used to pattern an array of digital nanodot gradients (DNGs), designed previously by our group using custom MatLab scripts [79]; the same DNGs are used in this work.

Other techniques to pattern proteins in nanometer-sized features include the use of AFM tips to perform dip pen nanolithography [80] and parallel dip pen nanolithography [81, 82], by selectively etching protein monolayers using low energy electron beam lithography [83], or using a nanopipette at the tip of a scanning probe microscope [84]. Most of these techniques require a large amount of time to pattern a small area of a surface, because the printing must be done in a direct write fashion. To produce a large surface area pattern, the writing tool must scan across the entire surface, which is time consuming. Furthermore, all of these techniques require very expensive pieces of equipment to perform the patterning. While parallel dip pen nanolithography does address the issue of slow patterning time, because multiple AFM tips in parallel are used to pattern large surface areas, it still requires the use of an expensive tool to perform this patterning. Low-cost nanocontact printing does not require any expensive equipment once the master mold is fabricated, and is able to pattern

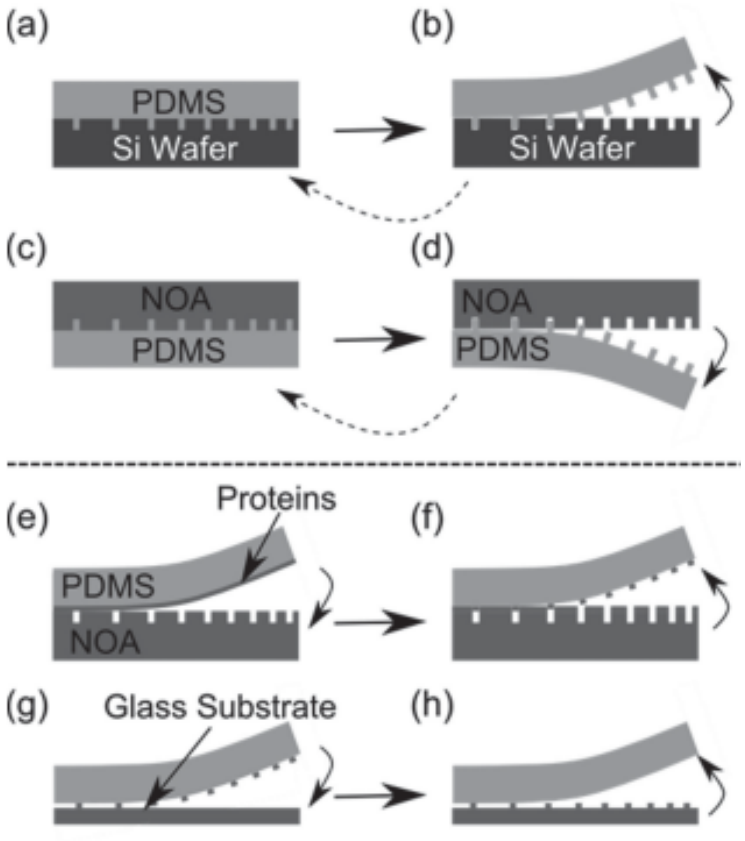

Figure 2.7: Low-cost nanocontact printing: in this adaptation of lift-off microcontact printing, a double replication step allows for an extended life span of the silicon master wafer, reducing the cost of the printing. Adapted from [1].

large surface areas with a single stamping step.

2.3 Effect of Substrate Stiffness on Cellular Behaviour

It has been known for many years that the mechanical properties of the cellular microenvironment can play a significant role in cellular behaviour. For example, changing the rigidity of a cell culture substrate can affect the differentiation of cells grown on that substrate. On very soft hydrogels, tuning the stiffness to below 1 kPa causes neural stem/progenitor cells (NSPCs) to differentiate into neurons, while gels with a stiffness above 7 kPa cause NSPCs to differentiate into oligodendrocytes [85]. Altering substrate stiffness has also been shown

to modulate the differentiation of mesenchymal stem cells into smooth muscle cells or chondrogenic cells following the application of TGF-β, with smooth muscle cells developing on stiff substrates and chondrogenic cells developing on soft substrates [86]. Other examples of substrate stiffness influencing cell differentiation showed osteogenesis on stiffer substrates, myogenesis on medium stiffness substrates, and neurogenesis on very soft substrates [87], or that stiffer hydrogels performed optimally for bone regeneration over softer hydrogels [88].

The idea that a cell receives information from its mechanical microenvironment has prompted the hypothesis that cells may actually 'feel' their way through organogenesis [89], showcased by such phenomena as the self assembly of shell-core cell aggregates between heart cells and retinal cells [90], and observations that external mechanical forces may induce or establish formation of symmetry axes during embryonic development [91]. While it remains difficult to fully decouple the influence of mechanical stimuli from biochemical stimuli in such cases, isolating the mechanical influence by altering substrate stiffness *in vitro* has been used as a tool for unraveling this phenomenon, and in this way substrate rigidity has been closely linked to altered cell phenotype (Figure 2.8) [2, 92], focal adhesion formation [2, 93], cell adhesion [89], and migration [94–96] – all key aspects of organogenesis and development.

It should be noted that biochemical and biomechanical stimuli are intrinsically linked - mechanical stimuli are transduced into chemical signals through the process of mechanotransduction [2], which subsequently leads to cytoskeletal rearrangement [97], and ultimately alteration of cell fate or cell behaviour. Numerous links have been made between mechanical stimuli and biochemical responses. It has been shown that nuclear lamin-A levels scale with tissue stiffness [98], and activation of lamin-A has been linked to matrix elasticity and myosin-IIA activation [99], making it a potential marker for extracellular tissue stiffness. Cytoskeletal responses to stiffness gradients include phosphorylation of the myosin-II heavy chain [100], and the alteration of cellular phenotype on different substrate stiffnesses is regulated by phosphotyrosine and Src family kinase signalling, leading to downstream cytoskeletal changes [97]. In addition, the frequency of transient filopodial calcium influxes in

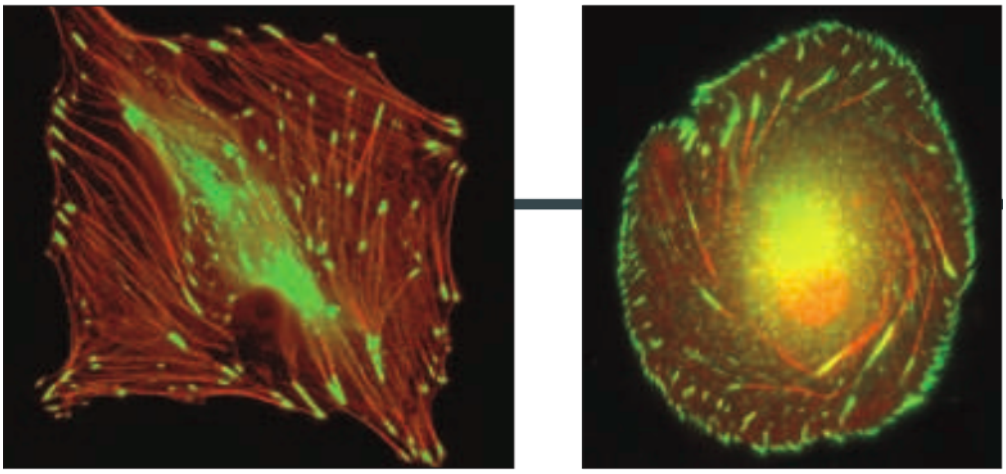

(a) Fibroblasts cultured on hard surfaces (100 kPa) are more spread, while those cultured on soft surfaces (10 kPa) are rounded. Adapted from [2].

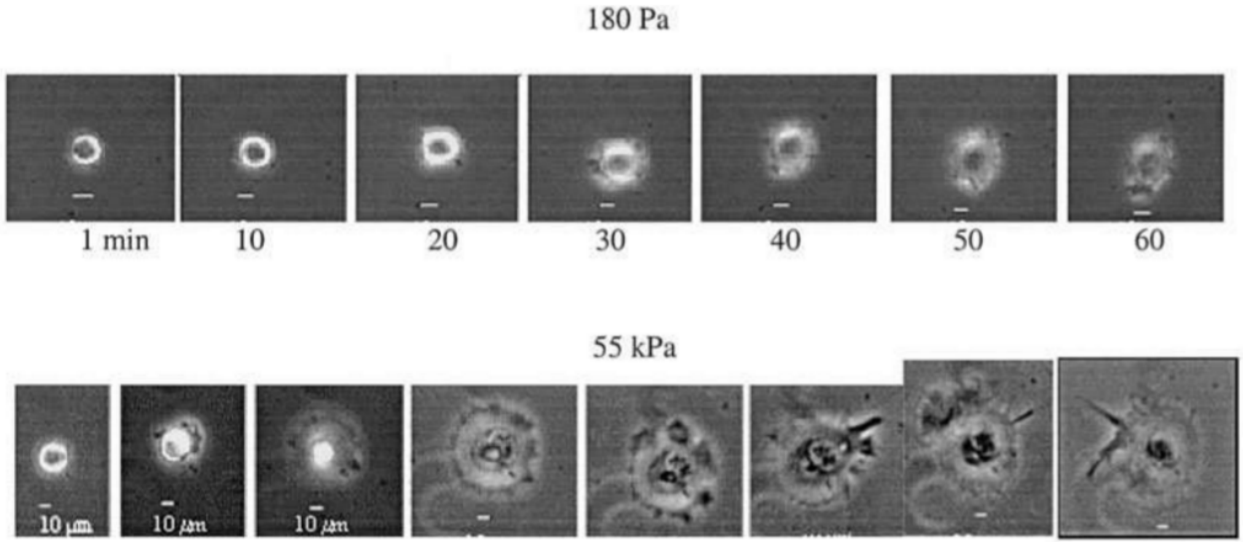

(b) A time series of NIH3T3 fibroblast phenotype on soft (180 Pa) and hard (55 kPa) substrates illustrates phenotypical differences. Adapted from [92].

Figure 2.8: Effect of substrate stiffness on cell phenotype

neuronal growth cones is modulated by substrate stiffness, possibly due to integrin receptor mediated calcium channels [101]. In the field of neuroscience, the mechanics of the cellular microenvironment have also been implicated in a wide range of cellular events pertaining to brain function, development, and plasticity, and there has been a call to increase our understanding of this influence of mechanical stimuli and forces, rather than relying solely

on biochemical studies [102, 103].

2.4 Altering Substrate Stiffness *in vitro*

To elucidate the relationship between substrate stiffness and cellular behaviour, it is necessary to isolate the substrate stiffness as a variable in an experimental setting. To this end, a variety of techniques and materials have been developed to alter the stiffness of cell culture substrates for *in vitro* assays.

2.4.1 Stiffness Gradients: Durotaxis and Migration Assays

Perhaps the most prevalent use of *in vitro* stiffness alteration has been the development of stiffness gradients for durotaxis assays. Durotaxis is a relatively recent term (first coined in 2000 [95]) which refers to preferential cellular migration towards a mechanically stiff substrate [104]. Migration towards substrates of lower stiffnesses is termed negative or reverse durotaxis [105, 106]. As a biological concept, durotaxis is relatively new, but it has already been implicated in embryo development, cancer metastasis, and wound healing [104, 107].

Durotaxis was first observed in 3T3 fibroblast cells cultured on flexible polyacrylamide sheets that were coated with type I collagen [95]. By generating a discontinuity in the concentration of the bis-acrylamide cross-linker during the generation of the sheets, two distinct regions were created, one with a high stiffness, and one with low stiffness. The discontinuity was created by placing a drop of the soft and hard acrylamide mixtures on either side of a coverslip, and spreading them with a second coverslip, such that they met in the middle. It was postulated that increased substrate rigidity resulted in an increase in cellular traction forces, which biased the cell movements towards the rigid substrate. Since that time, techniques for generating stiffness gradients have grown to include stiffness alterations within poly(ethylene glycol) (PEG) hydrogels [106], and photopolymerizable polyelectrolyte multilayers (PEMs), which can create stiffness gradients by selective degrees of photocuring [108].

Selective photopolymerizing was also used to make stiffness gradients using PEG diacrylate hydrogels with different polymer chain lengths [109]. Another group made stiffness gradients of collagen gel by simply varying the thickness of the gel on an underlying PDMS template [107]. A technique for creating sharply defined interfaces of stiffnesses, as opposed to a stiffness gradient, used the photoresist SU-8 to pattern squares of rigid photoresist on a pre-made layer of soft polyacrylamide gel [110, 111].

Different cell types have been used in durotaxis experiments, with varying results. Fibroblasts have been widely reported to display positive durotaxis [95, 107, 111], and rat aortic smooth muscle and human osteosarcoma cells demonstrated positive durotaxis on PEMs [108]. On the other hand, HT-1080 human fibrosarcoma cells displayed negative durotaxis, preferring stiffnesses of 100 Pa over 360 Pa on PEG hydrogels.

In addition to developing stiffness interfaces in two-dimensional cultures, a select few methods have attempted to introduce this concept into three-dimensional culture systems as well. Most notable is the use of a 3D culture chamber with microfluidic inlets, with which concentrations of hydrogel crosslinkers could be produced, resulting in a stiffness gradient within the chamber. This device was also proposed as a technique for investigating simultaneous application of 3D stiffness gradients overlaid with 3D chemical gradients [112].

2.4.2 Effect of Substrate Stiffness on Cell Phenotype and Differentiation

While some studies investigating the effects of substrate stiffness on cell behaviour utilise techniques to create a gradient of stiffness within the culture dish, other studies simply alter the stiffness of the substrate for an entire experiment, and compare cell behaviour between dishes with substrates of different stiffnesses. The techniques for creating these conditions are usually more simple, as the technical requirement of generating a gradient is removed, and the only requirement is a material with a tuneable stiffness that is compatible with cell culture; many of the same materials are used for these experiments as were mentioned before.

Hydrogels are commonly used for these purposes, such as agarose [3] or polyacrylamide gels [4, 113], as well as polyeletrolyte multilayers, for example made with alternating layers of poly-L-lysine and hyaluronan [114]. Common findings are that migratory cells such as fibroblasts will spread out more and move less on stiffer substrates, indicative of stronger adhesion to stiffer substrates [2, 108, 114, 115]. However, this is not necessarily indicative of better cell growth, when viewed in the context of cellular differentiation, as optimal cell differentiation occurs on substrates with stiffnesses close to the stiffness of the *in vivo* origin tissue [87, 113]. This indicates that the preferred or optimal substrate stiffness is cell type dependent, and that the optimal stiffness is close to the *in vivo* microenvironment stiffness that a particular cell type would encounter. To further this train of thought, it has been observed that increased neurite outgrowth [3, 116] and branching [4] occurs on softer gels rather than harder gels, a result which may be indicative of increased neurite health on the softer substrates that more closely recapitulate the *in vivo* stiffness of the brain [117,118].

Other studies used formulations of PDMS to attain different substrate stiffnesses. In one study, mouse embryo development was compared between three cases: polystyrene petri dishes (E = 1 GPa), PDMS (E = 1.8 MPa), and collagen gels (E = 1 kPa). Development on PDMS and collagen gels was significantly improved when compared to the petri dishes, and implantation studies with the embryos after a period of *in vitro* culture showed that the pre-implantation culture conditions had lasting impact on the fetuses, as the embryos from softer substrates had larger placentas throughout development [119]. Another common method of varying substrate stiffness is to change the ratio of base to curing agent in PDMS substrates, which enables the elastic modulus to be tuned. Dorsal root ganglion neurons and glial cells were found to develop differently on PDMS substrates of differing stiffnesses [120], and PDMS substrates were used to investigate how mechanosensitive TRPC1 channels regulate neuronal growth cone development through transient calcium influx [121]. Even softer versions of PDMS are made by using different monomers – Sylgard 527 is a commercially available PDMS formulation with an elastic modulus < 10 kPa [5], and it has been used

to demonstrate that physiologically representative substrate stiffnesses can regulate primary hepatocyte function [7], to probe the mechanosensitivity of PC12 neurite extension and C2C12 myoblast differentiation [9], and to investigate the effect of substrate stiffness on corneal endothelial expansion [8].

2.5 Integrating Mechanical and Biochemical Signals

It has been widely reported that a variety of extracellular factors mediate cellular migration, such as biochemical signalling molecules and the mechanical properties of the extracellular micro-environment, as discussed above. In addition to these, other factors have been shown to influence cell motility *in vitro*, from electrical signals causing alignment and migration of fibroblasts (a process known as electrotaxis) [122–124], local topographical landmarks [125–127], externally applied mechanical forces [91, 128–131], and even light sources [132,133]. While techniques have been developed to elucidate the processes by which each of these external cues influences cell motility, there has been comparatively little focus on the influence and interplay between these different signals. Some studies which have focused on the integration of multiple different types of external cues investigated the synergistic effects that local topographies and chemical gradients can have on neurite outgrowth [126], or have developed techniques to pattern proteins on topographically complex substrates [134]. While these examples are a step towards understanding the integrated effects of multiple types of extracellular cues on cell migration, these are some of the only examples in the literature. Thus it is evident that there is still a great body of work to be done to more fully understand the interplay between multiple cues in a biological system.

2.5.1 Biochemical Migration Assays: Integration with Mechanically Compliant Substrates

Examples of studies which examine the interplay between chemically guided motility and substrate stiffness include a study which examined chemotaxis of neutrophils on compliant hydrogel substrates [135], and a study that found that the stiffness of an agar gel affected the chemotactic behaviour of bacteria [136]. The effect of substrate stiffness on chemotaxis can be intuitively seen as an extension of the effect that the substrate stiffness has on cell motility. In the presence of a biochemical cue, any alterations to cell motility will be inherently translated into the ability of the cell to respond to this cue. This relationship has been investigated through mathematical modelling of chemotactic cells on elastic substrates [137].

However, despite observations that altering substrate stiffness can impact chemotactic behaviour, no studies to date have investigated the effect of substrate stiffness on haptotactic behaviour. In order to perform this investigation, it is first necessary to develop novel techniques to pattern substrate bound proteins on substrates of varying stiffnesses. To this end, in recent years there have been several examples of surface bound protein patterning on mechanically diverse and compliant substrates, which are discussed here. One technique used poly(N-isopropylacrylamide) as an intermediate film in an adapted version of micro-contact printing to enable patterning on topographically complex surfaces [134]. Other techniques use poly(vinyl alcohol) thin films [6] or layers of dextran [138] as sacrificial layers to enable protein patterning on soft or complex surfaces (Figure 2.9). Patterning on hydrogels has been accomplished by freeze drying the hydrogel before using standard micro-contact printing on the surface, followed by reconstitution of the gel and use with cell culture [139]. A common theme with each of these techniques is that some extra step is required – either a sacrificial film, or a reversible hardening of the substrate – in order to adapt conventional protein patterning techniques to the softer substrate. Notably, despite claims that these techniques are adaptable for patterns into the nanometer range of feature sizes [6, 138], none of them demonstrate patterning of nano-scale feature sizes. Furthermore, none of these techniques

demonstrate patterning of surface bound protein gradients such as DNGs, and none of these techniques have been used to investigate the effect of substrate stiffness on guided cellular migration via haptotaxis.

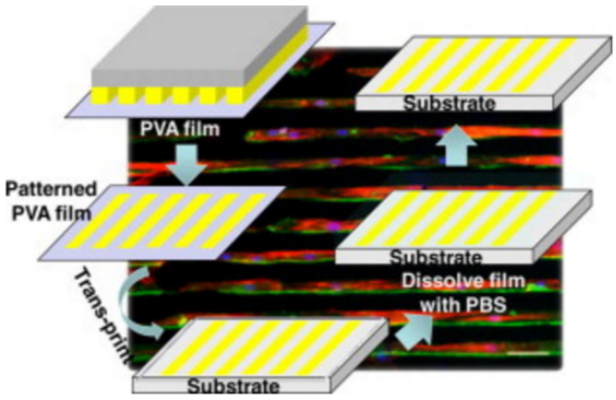

(a) Microcontact printing on soft substrates using dissolvable PVA films. First the protein pattern is printed on a PVA film, which is then inverted and placed on the soft substrate, and finally dissolved with PBS, leaving the protein pattern behind. Adapted from [6].

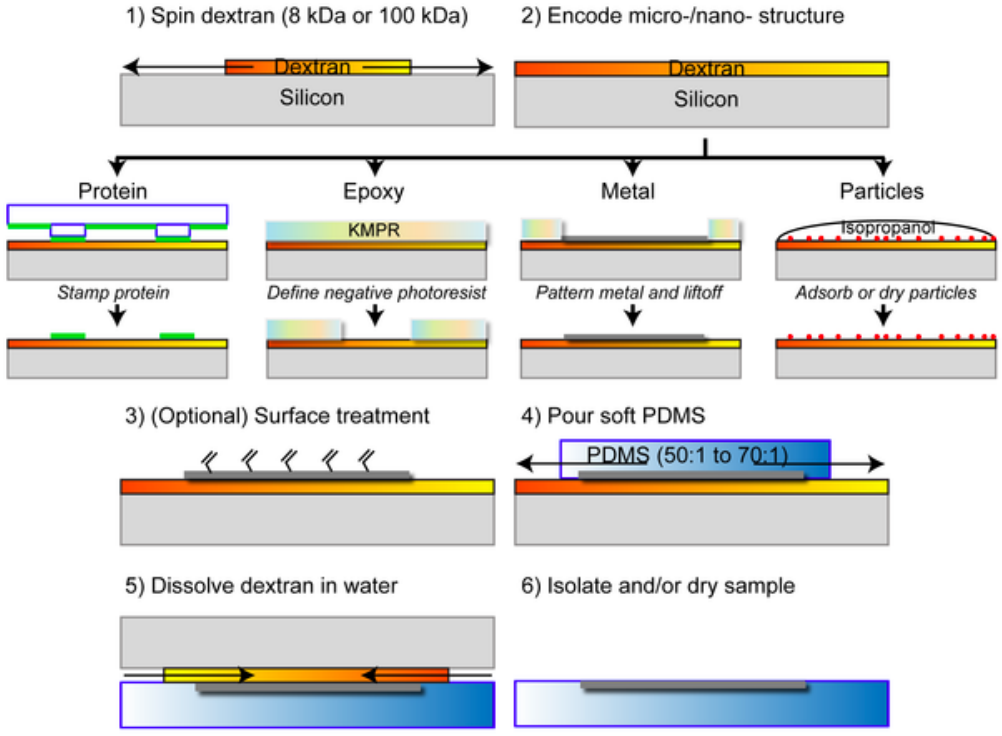

(b) Microcontact printing on soft substrates using dissolvable dextran. Proteins may be patterned on dextran, and soft PDMS is cured on top of the protein patterns. The dextran is then dissolved, releasing the soft PDMS with the protein pattern. Adapted from [138].

Figure 2.9: Adapting microcontact printing to soft and tacky substrates.

3 Nanocontact printing on soft substrates: haptotaxis on netrin-1 digital nanodot gradients

This chapter is presented in manuscript form. The manuscript is currently under internal review by the authors, however the intention is to submit this manuscript for publishing in the near future.

Nanocontact printing on soft substrates: haptotaxis on netrin-1 digital nanodot gradients

Donald MacNearney, Bernard Mak, Timothy E. Kennedy, David Juncker

McGill University, Montreal, Canada

Abstract

Surface bound gradients of guidance cues are important for directing cellular processes during development and repair. *In vivo*, these gradients are presented in the mechanically soft extracellular matrix, but *in vitro* haptotaxis experiments to date have been conducted primarily on hard substrates. Here, a technique is presented for patterning haptotactic proteins on soft Sylgard 527 substrates (E $<$ 10 kPa) with nanometer resolution. A lift-off nanocontact printing technique was developed using dissolvable thin films of poly-vinyl alcohol to pattern substrates without using plasma activation, which was found to alter the substrate's mechanical properties. An array of 100 unique digital nanodot gradients (DNGs), consisting of millions of 200$\times$200 nm^2 protein nanodots, was patterned in less than 5 min. DNGs were successfully replicated with $<$ 5% average deviation from the original gradient design. DNGs of netrin-1 – a known protein guidance cue – were patterned and the un-patterned surface was backfilled with a reference surface consisting of 75% poly-ethylene glycol grafted with poly-lysine and 25% poly-D-lysine. Haptotaxis of C2C12 myoblasts demonstrated the functionality of the DNGs patterned on soft substrates. High densities of netrin-1 were observed to induce cell spreading, while live imaging of cell migration on sinusoidal gradients highlighted cell navigation by 'inching'. The nanopatterning technique developed here, and the subsequent experiments on digital nanodot patterns, may be expanded for use with primary cells, such as neutrophils and neurons.

Preprint submitted to Biomaterials *June 17, 2016*

3.1 Introduction

Cellular navigation, migration, and motility are vital requirements for life, whether it be during the development of an organism, or throughout the life cycle - for example during tissue maintenance and wound healing. This process is regulated by continuous integration of multiple extracellular cues. Surface bound chemical cues regulate cell navigation in neutrophils, myoblasts, and developing neurons through a process known as haptotaxis.

Haptotaxis is defined as directed cell motility or outgrowth mediated by surface bound navigational cues. Early experimental demonstrations of haptotaxis include guided axon projection of retinal axons on surface bound continuous gradients of proteins derived from the optic tectum [33, 34, 140], and directed locomotion of murine myoblasts on laminin carpets [141]. More recently, digital gradients of surface bound cues have been used to study haptotaxis in axon development, using a modified microcontact printing (µCP) process [59] to pattern surfaces with digital spots of substrate bound ephrinA5 [60]. A variation of this printing process was used to pattern digital nanodot gradients (DNGs) of surface bound proteins, consisting of 200×200 nm^2 protein dots, to investigate C2C12 myoblast migration on gradients of netrin-1 [1].

Netrin-1 is a well documented axon guidance cue [39], however it is also present in a variety of systems outside the nervous system [142]. C2C12 myoblasts express the netrin-1 receptor Neogenin [45], making these cells an attractive model to use for developing netrin-1 gradient assays that may also be applicable to axon turning studies.

A common feature of the above examples of haptotaxis is that most protein gradients were generated on glass or polystyrene surfaces. Both glass and polystyrene have elastic moduli in the GPa range, which is much stiffer than the typical moduli of biological tissues (Figure 3.1). The gradients developed by Baier and Bonhoeffer [33] were generated on capillary pore filters rather than glass, but the elastic modulus of the substrate in these assays

was not assessed. In recent years, the importance of the mechanical properties of the cellular microenvironment has been realised, and it has been noted that the elastic modulus of the substrate can have a large impact on a broad range of cellular processes, including cellular motility and migration [94, 95]. For example, the stiffness of compliant hydrogel substrates was found to have an impact on the chemotactic behaviour of neutrophils [135] and bacteria [136]. Despite these findings, to date there have been no reports addressing the effect of cell culture substrate stiffness on cellular haptotaxis.

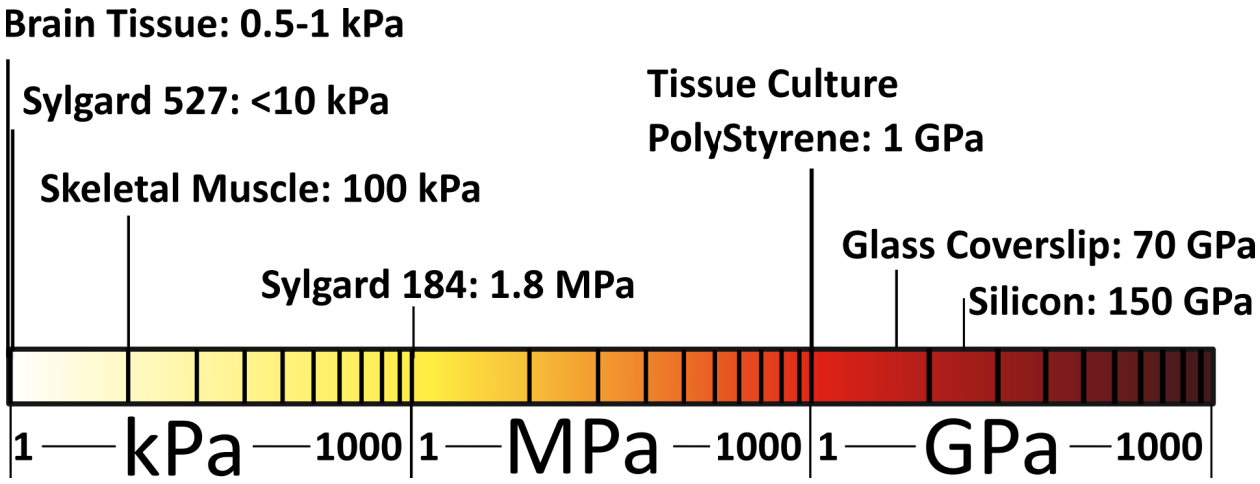

Figure 3.1: Elastic moduli for conventional cell culture substrates, two forms of PDMS (Sylgard 184 and Sylgard 527), and two biological tissues. Silicon included for reference.

Soft and tuneable substrate stiffnesses have been achieved *in vitro* using a variety of techniques, such as varying the cross-linker concentration in agarose [3] and polyacrylamide gels [4, 113]. While many of these substrates are made using hydrogels, it is also possible to fabricate soft substrates of silicone by tuning formulations of poly(dimethyl siloxane) (PDMS) to different stiffnesses – in this work silicone substrates are used. The stiffness of PDMS substrates may be tuned by varying cross-linker concentrations, or by mixing commercial formulations of PDMS with different stiffnesses [5, 7–9, 120, 121]. Sylgard 184 and Sylgard 527 – stiff and soft formulations of PDMS, respectively – are commonly used for these purposes.

Recently, protein patterning on soft formulations of PDMS has been demonstrated using variants of µCP. Traditional µCP is not compatible with soft substrates because of deformations and surface defects that arise during the process, resulting in poor quality patterns. In addition, µCP involves plasma activation of the final substrate. Exposure of PDMS to long plasma treatments has been shown to alter the mechanical stiffness of PDMS substrates, which is detrimental when the substrate is desired to have a predictable and repeatable stiffness [143]. To enable protein pattern transfer to soft substrates without surface deformations or plasma activation, sacrificial intermediate films have been used, made from poly(vinyl alcohol) (PVA) [6] or dextran [138]. Using these techniques, the highest resolution protein patterns made on soft surfaces to date were 2 µm in size [6].

Here, we present a novel process for large scale patterning of nanometer size features onto soft substrates. In this work, Sylgard 527 was selected as an soft material because it has a very low elastic modulus (<10 kPa [5]) (close to that of *in vivo* brain tissue [117, 144, 145]) and because it has previously been used as a soft material for *in vitro* studies [6–9]. Our protein patterning technique was used to generate DNGs of surface bound proteins on soft substrates for use in haptotaxis assays. C2C12s were seeded on DNGs of netrin-1 to evaluate the bio-functionality of the patterned gradients.

3.2 Materials and Methods

3.2.1 Preparation of PVA Films and PDMS Stamps and Substrates

Thin films of PVA were made by mixing 1.5 g of PVA powder (Sigma-Aldrich, Oakville, ON, Canada) with 40 ml of distilled water and dissolving the powder by microwaving the beaker in a 700 W microwave for two minutes at 50% power, with occasional stirring. When the powder was fully dissolved the solution was poured into a large petri dish and allowed to cool and dry for 1-2 days. Once the film was fully dry, it was cut with a scalpel into small squares and used as necessary for printing on Sylgard 527.

Sylgard 184 (Dow Corning, Corning, NY, USA) was mixed as per the manufacturer's instructions at a 10:1 ratio of base to curing agent, degassed in a vacuum chamber for 30 minutes, and poured onto a large petri dish, forming an even layer approximately 0.5 cm thick. This was cured overnight in a 60 °C oven (VWR, Montreal, QC, Canada), after which small squares could be cut and used for nanocontact printing.

Soft substrates were fabricated using Sylgard 527 (Ellsworth Adhesives, Germantown, WI, USA), which was mixed as per the manufacturer's instructions at a 1:1 ratio between components A and B. After thorough mixing, 75 µm layers of Sylgard 527 were formed on glass bottom dishes by placing a 200 µl drop in the center of the dish and spincoating at 500 rpm for 15 s. Alternatively, drops of liquid pre-polymer were allowed to spread without spincoating on pieces of glass slide or glass bottom dishes, resulting in thicker layers that were slightly convex, but which were nonetheless still useable for experiments. The coated glass slides and glass bottom dishes were cured overnight in a 60 °C oven (VWR, Montreal, QC, Canada), after which they were soaked in 70% ethanol for over six hours to extract unpolymerized monomers. Ethanol was removed and the substrates were dried in the 60 °C oven to evaporate excess ethanol.

3.2.2 Young's Modulus Measurements

Samples of Sylgard 527 were prepared on glass slides as above. Samples were plasma treated (PlasmaEtch PE-50, PlasmaEtch, Carson City, NV, USA) for up to 60 s, after which an atomic force microscope (AFM) (Asylum Research, Santa Barbara, CA, USA) was used to perform indentation measurements. A custom Matlab code was used to extract the Young's modulus from the measured displacement curves.

3.2.3 Gradient Design and Electron-Beam Lithography

The DNGs used in this work were previously presented in Ongo *et al.* [79]. Briefly, a custom MatLab script was used to generate digital nano-dot gradient designs that were subsequently imported into L-Edit for assembly into a wafer scale digital design file. E-beam lithography (VB6 UHR EWF, Vistec, Montreal, QC, Canada), followed by reactive-ion etching (System100 ICP380, Plasmalab, Everett, WA, USA) was used to pattern the nanodot gradient arrays on a 4" silicon wafer, at a depth of 100 nm. The wafer was silanised with perfluorooctyltriethoxysilane (Sigma-Aldrich, Oakville, ON, Canada) using vapour phase deposition.

3.2.4 Gradient Array Replica Molding

The master wafer pattern was recreated using a double replication process, using PDMS (Dow Corning, Corning, NY, USA) and then a UV curable polyurethane (Norland Optical Adhesive 63 (NOA 63), Norland Products, Cranbury, NJ), as described in Ricoult *et al.* [1]. First, PDMS was mixed at a 10:1 ratio of base to curing agent, degassed in a vacuum dessicator, and poured on the wafer in a petri dish. The PDMS was then cured at 60 °C, and was cut and peeled off the wafer. A small volume of NOA was poured over the gradient pattern on the PDMS replica, and cured with 600 W of UV light (Uvitron International Inc., West Springfield, MA, USA) for 30 s. The cured NOA was removed from the PDMS, yielding a replica of the pattern on the silicon wafer, consisting of 200×200 nm^2 holes making up a digital gradient array.

3.2.5 Nanocontact Printing

Protein solution was inked onto a flat piece of PDMS about 1×1 cm^2 square for about 5 min. The concentration of the inking solution varied – for netrin-1 prints, recombinant netrin-1 (produced and purified as described [146, 147]) was diluted to 25 µg/ml with the

addition of a fluorescent dye at 10 µg/ml for visualization, while control prints consisted of just the fluorescent dye at 10 µg/ml. All proteins were diluted in phosphate buffered saline solution (PBS). The flourescent dye used for visualization and controls was goat-anti-rabbit immunoglobin-G (IgG) conjugated with Alexa-Fluor 546 dye (Invitrogen, Burlington, ON, Canada). The protein solution was spread across the surface of the flat stamp by placing a small coverslip on top of the drop of solution. After incubation, stamps were rinsed briefly with PBS and MilliQ water before being dried gently under a stream of nitrogen. Plasma activated (PlasmaEtch PE-50, PlasmaEtch, Carson City, NV, USA) NOA replicas of the DNG pattern were brought into contact with the dried stamp, and the stamp was then pressed onto either plasma activated glass, in the case of printing on glass, or onto a thin film of plasma activated PVA, in the case of the printing on Sylgard 527. For printing on Sylgard 527, the PVA film was then inverted and gently contacted with the surface of the Sylgard 527 sample. Both glass and Sylgard 527 samples were hydrated with PBS at this point. After 1-3 min the PVA film was floating in the PBS and could be removed with tweezers.

3.2.6 Reference Surface

After the print was patterned onto either glass or Sylgard 527, the coating of PBS was aspirated with a pipette and replaced with reference surface (RS) solution, consisting of 10 µg/ml poly-D-lysine (PDL, 70-150 kDa, Sigma-Aldrich, Oakville, ON, Canada) and 10 µg/ml poly-L-lysine (PLL) conjugated with polyethylene glycol (PEG) (PLL(20)-g[3.5]-PEG[2], Surface Solutions, Dübendorf, Switzerland), mixed at a ratio of 25% to 75% (v/v), respectively. The reference surface was left on the substrate at 4 °C for an incubation period of 1 or 3 h before being aspirated, after which the substrate was rinsed with PBS.

3.2.7 Cell Culture and Haptotaxis Assays

C2C12 myoblast cells (ATCC, Manassas, VA, USA) were cultured in 25 cm^2 cell culture plates in media consisting of high glucose DMEM supplemented with 10% fetal bovine serum

and 1% penicillin/streptomycin (Invitrogen, Burlington, ON, Canada). Cells were passaged every 2-3 days into a new flask, and excess cells seeded onto DNGs patterned on Sylgard 527, at a density of 2500 cells/cm^2. Cells were kept in a cell culture incubator at 37 °C with 5% CO_2 for 18 h before imaging.

Cells were fixed in 4% paraformaldehyde with 0.2% (v/v) gluteraldehyde solution (Sigma-Aldrich, Oakville, ON, Canada) for 4 min. Cells were either imaged using bright field optics at this point or stained for fluorescence imaging. Cells to be stained were permeabilized with triton-X 100 for 4 min, and blocked with horse serum for 1 h. Cells were labelled with phalloidin conjugated to Alexa Fluor 488 (1:250, Invitrogen, Burlington, ON, Canada) and with Hoechst stain (1:10,000, Invitrogen, Burlington, ON, Canada).

3.2.8 Image Quantification and Data Analysis

Images of cells and gradients were overlaid using ImageJ, and the geometric center of each cell was marked using the multi-point tool. The angle and origin of each gradient was also marked, and all of this data exported to a custom MatLab script to normalize the data points onto a single axis, representative of a DNG. Cell populations were merged across gradients for each experiment, and variations from an even distribution across gradients were detected using the Student's t-test.

3.3 Results and Discussion

3.3.1 Brief Plasma Exposure Physically Alters PDMS

In traditional µCP, the final substrate is typically plasma activated to ensure high quality transfer of the protein pattern. The process of plasma activation, however, can significantly alter the surface characteristics of certain materials. It is well known that lengthy plasma activation of PDMS substrates, such as the Sylgard 527 used in this work, results in the formation of a surface layer of glass that has different mechanical properties from the bulk

PDMS substrate [143, 148]. In certain scenarios this surface modification can lead to buckling and topographical alterations [149–152].

We tested whether plasma activation for short exposure times could facilitate protein transfer, but without significantly affecting the substrate properties. Samples of Sylgard 527 were plasma activated for up to 60 s, and the surface stiffness was measured by indentation with an AFM tip (sample deflection curves may be seen in Figure S3.1). Samples were also submerged in PBS to replicate the hydrated environment required for cell culture on these surfaces. Finally, nanocontact printing was used to pattern DNGs on plasma activated Sylgard 527. While the surface of the Sylgard 527 was originally flat and smooth (Figure 3.2(a)), plasma activation for even as little as 10 s gave rise to long cracks across the surface. Buckling of the surface around these cracks did not appear until the samples were hydrated (Figure 3.2(b)). The observed buckling patterns appear consistent with water induced swelling of the PDMS substrate, which buckles the newly formed glass layer on the surface [152]. Increased plasma time results in less of these buckling patterns, but more pronounced surface cracks, possibly indicating the formation of a more stiff and uniform glass layer that resists buckling (Figure 3.2(c)). Protein patterning on plasma activated Sylgard 527 resulted in visible cracking of the pattern, due to the breaking and shifting of the glass layer formed during plasma treatment (Figure 3.2(d)).

Using AFM indentation measurements, it was found that increasing lengths of plasma activation increased the Young's modulus of the Sylgard 527, from kPa to MPa range. It should be noted that the measurements made on plasma activated Sylgard 527 were subject to large variations, reflected in the standard deviation values, which we interpret as indicative of a heterogeneous surface. While it may be possible to plasma activate Sylgard 527 and not change the modulus (as in the 10 s case), the increased standard deviation indicates that some areas have hardened, and thus the surface is less uniform. From these experiments, we conclude that even short plasma exposure times can significantly alter the mechanical properties of Sylgard 527. Further, these alterations may vary locally, owing to

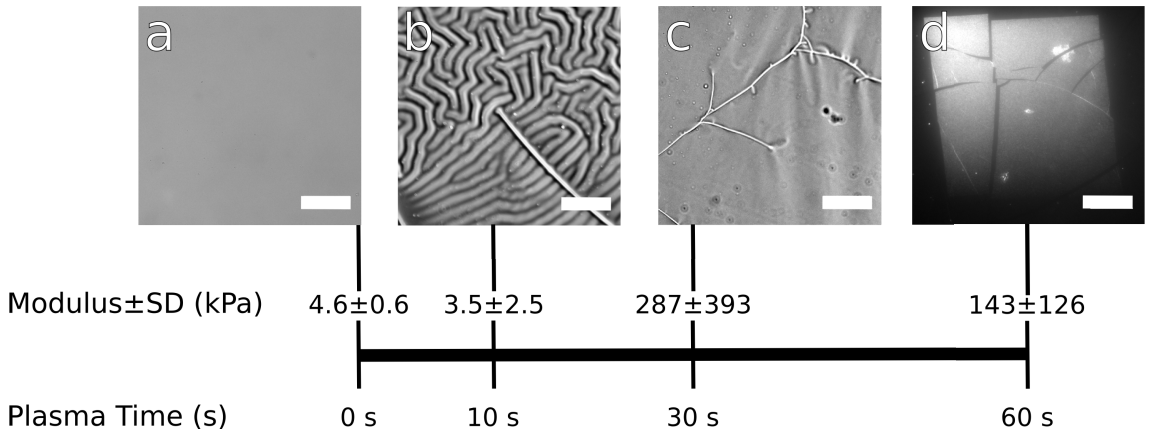

Figure 3.2: Effect of plasma treatment on Sylgard 527. a) Unactivated Sylgard 527 appears smooth under bright field microscopy. b) Plasma activation for 10 s increases the variability of the elastic modulus as measured using AFM indentation, indicating non-uniform hardening of the surface, while some large cracks form across the surface. Hydration of the sample results in ordered buckling patterns across the surface, consistent with water induced swelling at the glass/PDMS interface. c) Plasma activation for 30 s results in a large increase in elastic modulus and the formation of a larger network of surface cracks. Hydration of the sample results in surface buckling but to a lesser degree. d) Fluorescence micrograph of a substrate that was patterned by nanocontact printing after 60 s plasma. The high fluorescence shows that the proteins were successfully transferred to the substrate, while large cracks on the surface are reminiscent of broken glass, suggesting that printing broke the plasma induced glass layer at the surface of soft PDMS. Scale bars are 100 µm.

inhomogeneous plasma in the chamber, and may vary from day to day due to overall plasma power variation. Thus for experiments that require well defined mechanical properties of the substrate, plasma activation is inappropriate.

3.3.2 Patterning Digital Nanodot Gradients on Soft Substrates

DNGs were designed as described in Ongo *et al.* [79] and in Ricoult *et al.* [1]. Briefly, a 10×10 array of DNGs was fabricated on a silicon wafer using e-beam lithography, with each gradient being 400×400 µm^2, and consisting of many thousands of 200×200 nm^2 squares. The surface density of the squares was varied along each gradient to match a programmed density profile (Figure S3.2). The array contains gradients with linear and exponential den-

sity profiles, with random and ordered dot placements within these profiles. A large subset of gradients also vary their nanodot densities sinusoidally within a linear or exponential envelope. The patterning method shown by Ricoult *et al.* was modified to permit patterning on soft substrates, such as Sylgard 527.

The biggest challenge with printing on soft substrates is that removal of the stamp from the substrate can rip and tear the surface of the substrate. To overcome this challenge, thin films of water soluble PVA were used as an intermediate medium in a novel printing process. First, a flat PDMS stamp was inked with protein and contacted with a plasma activated NOA template containing the nano-pattern (Figure 3.3(a-b)). Undesired protein adsorbed to the NOA template, leaving behind the nano-pattern on the PDMS stamp. The stamp was then brought into contact with a plasma activated film of PVA, transferring the nano-pattern to the film (Figure 3.3(c-d)). The film of PVA was inverted and contacted with the soft substrate (Figure 3.3(e-f)). As PVA is water soluble, submersion in PBS for several minutes caused the PVA film to partially dissolve and spontaneously detach from the substrate to float in the solution (Figure 3.3(g-h)). The PVA was then picked up and discarded using tweezers. This process circumvented the need to manually peel the stamp away from the soft surface, and a print could be completed in $\sim$5 min.

In this process, the protein transfer from the PVA film to the Sylgard 527 is mediated by similar molecular interactions to those seen in humidified microcontact printing (HμCP) [78]. In HμCP, protein transfer to low surface energy substrates is facilitated by plasma activation of the stamp, rather than the substrate, and by the addition of water. Water molecules will tend to interact with the higher surface energy of the stamp, forming a thin layer of water between the protein and the stamp and desorbing the protein. In this environment, it is postulated that hydrophobic interactions will promote transfer of the protein to the hydrophobic target substrate, akin to the spontaneous adsorption of protein on hydrophobic surfaces from solution. Thus, in the printing technique demonstrated here, the addition of PBS performs two roles - the detachment of the PVA film from the Sylgard 527 by partially

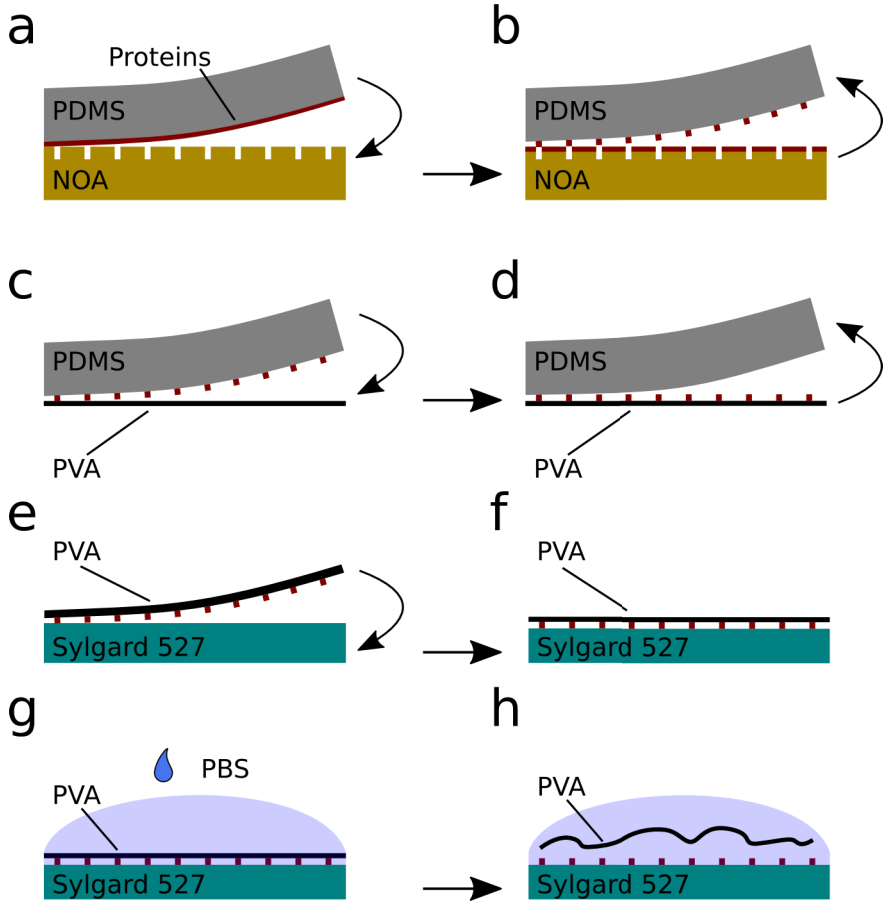

Figure 3.3: Process flow diagram for nanocontact printing on soft and tacky surfaces, such as Sylgard 527. (a-b) A flat PDMS stamp (Sylgard 184) is coated with protein and contacted with plasma activated NOA containing a relief of the desired nanodot pattern. Undesired protein sticks to the NOA upon stamp removal. (c-d) The pattern is transferred to a plasma activated PVA film. (e-f) The PVA film is gently laid onto Sylgard 527. (g-h) The print is hydrated with PBS until the PVA film partially dissolves and floats in the solution, after which it may be removed with tweezers.

dissolving it, as well as the facilitation of protein transfer to the hydrophobic Sylgard 527.

Using the technique shown in Figure 3.3, it was possible to replicate DNGs on Sylgard 527. Images of the printed gradients on glass and Sylgard 527 were overlaid with the original design file for comparison of pattern fidelity and reproducibility (Figure 3.4). An ordered gradient with a linear density slope of 0.01%/µm was selected for this evaluation. Denoted by the arrows in Figure 3.4(b), pattern skewing is evident on Sylgard 527. This skewing

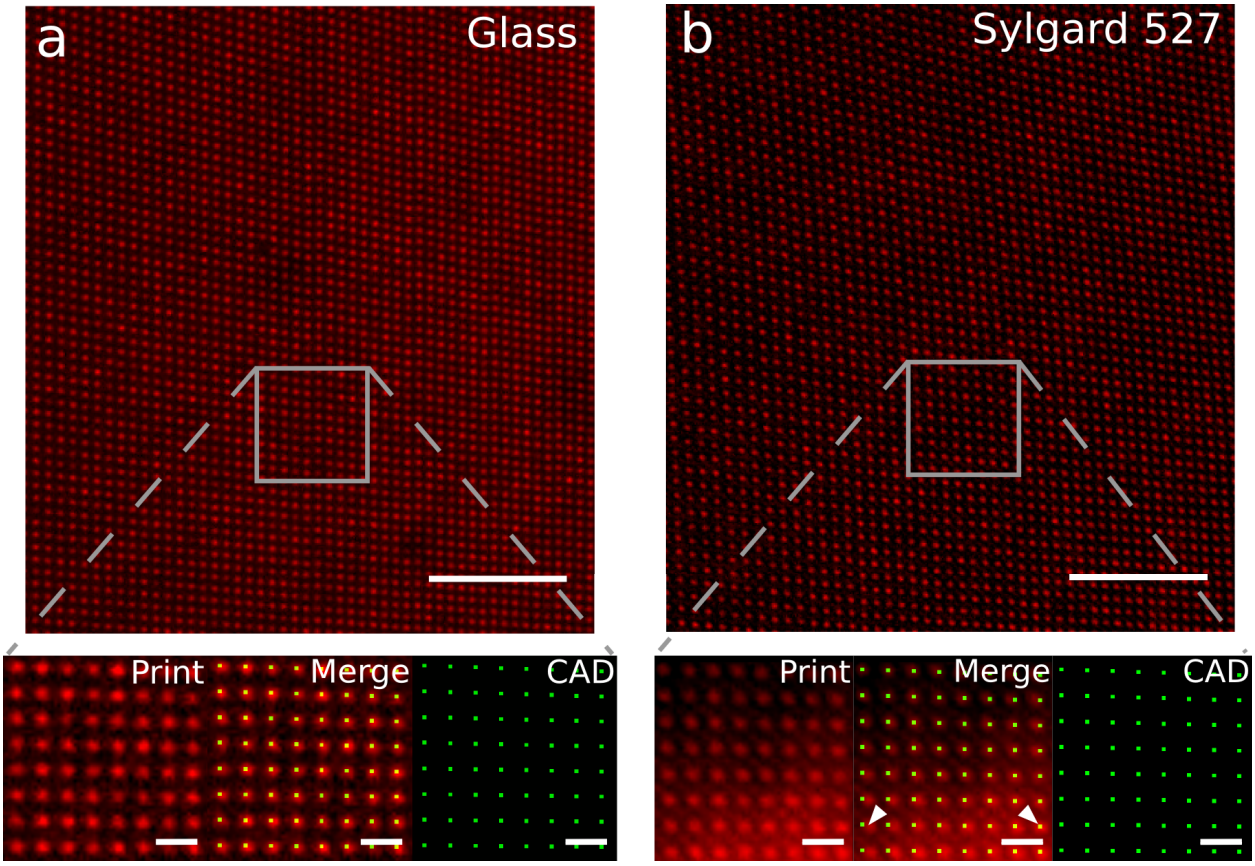

Figure 3.4: Fluorescence micrographs of DNGs patterned on Sylgard 527 and glass substrates. An ordered linear gradient, with a density slope of 0.01%/µm, patterned on a) glass and b) Sylgard 527. Insets show enlarged image of the print, the original CAD file of the same area, and a merge of the two. In a), the merged image indicates near perfect overlap between the print and the design file, while in b) skewing is visible due to a mismatch between the pattern and the CAD. Arrows denote where the measurements were taken; the right arrow indicates a zone where printed and CAD patterns are aligned, and the left arrow shows the print deviating from the design file by 0.40 µm over a total distance of 8.64 µm. Scale bars are 15 µm for the large images and 2 µm for the insets.

varied between samples, and was manifested in the prints as either a compression or an extension of the pattern. In Figure 3.4(b), the mismatch between the pattern and the CAD design was 0.40 µm over a distance of 8.64 µm, or 4.6%. Quantification of skewing over multiple gradients revealed an average skewing (either extension or compression of the pattern) of 4.25% (n = 115 gradients, 3 prints; SD: 4.0%). We attribute the skewing to the deformation of the soft Sylgard 527 substrate upon manually contacting it with the flexible

thin films of PVA during printing. The local deformation of the pattern will also induce a local change in surface density of the gradients, which may be calculated using Equation 1 [79].

$$D = \frac{A_{dot}}{{d_i}^2} \tag{1}$$

For an arbitrary square containing a single protein nanodot, the protein surface density is the area of the protein nanodot (A_{dot}) divided by the area of the square (${d_i}^2$). Uniaxial extension of the pattern, as seen in Figure 3.4(b), by the previously calculated average skewing of 4.25% manifests as an increase in d_i, and results in a local protein surface density decrease of 6.1%. Conversely, uniaxial compression decreases d_i; if skewing of 4.25% is assumed, the local protein density increases by 4.4%. In a worst case scenario, if biaxial extension and compression are assumed, these values change to 8.0% and 9.1%, respectively. Prints with large degrees of skewing were discarded, and whereas local skewing was tolerated to within 10%, on average the gradients matched closely with the design.

3.3.3 Reference Surfaces on Sylgard 527

When PDMS is used as a cell culture substrate, cell adhesion can be promoted by coating the substrate with extracellular matrix proteins such as fibronectin or collagen, or with charged molecules such as poly-L-lysine (PLL) [7, 121, 153, 154]. For haptotaxis assays, it is critical to tune the 'un-patterned' reference surface (RS) to provide a proper context for cells to make a choice between the patterned cue and the RS [27]. We previously introduced a system to systematically vary the RS by coating the un-patterned substrate with a mixture of variable ratios of poly-D-lysine (PDL) and poly(ethelyne glycol) grafted to a poly-L-lysine anchor (PEG-g-PLL), which exposes the grafted PEG groups upon adsorption to a surface [47]. PDL is known for its ability to promote cell adhesion, while PEG does not allow for cell adhesion, and thus by mixing the two polymers at various ratios and ad-

sorbing them to a substrate, a range of reference surfaces may be made. In this work, we tested whether the RS molecules would adsorb on Sylgard 527 as they do on glass substrates.

RS coverage on Sylgard 527 was tested using fluorescently labelled PLL and PEG-g-PLL molecules, under the assumption that the fluorophore does not markedly alter the adsorption properties. No significant differences were observed in the fluorescence levels between Sylgard 527 and glass substrates (Figure S3.3(a-b)). Plasma activating the substrate for 1 min increased the fluorescence levels on Sylgard 527, consistent with electrostatic interaction between the negatively charged silanol groups on the glassy layer atop the PDMS and the positively charged amine groups of the PLL. Adsorption did not change significantly when incubation times were increased from 1 h to 3 h (Figure S3.3(c-d)). For both unmodified and plasma activated Sylgard 527, while there was a large degree of variation in fluorescence levels between samples, the fluorescent coatings were found to be largely uniform across the surface of individual samples, and no sample was found to be uncoated (Figure S3.4). We concluded that PLL and PEG-g-PLL adsorbed reliably on Sylgard 527 without need for plasma activation.

3.3.4 Haptotaxis Assay on Soft Substrates

The DNGs used in this work were designed for use in a cellular haptotaxis assay (Figure 3.5(a)). For this assay, DNGs of netrin-1 were patterned on the soft PDMS using the printing technique in Figure 3.3, and the surface was then backfilled with a RS. The RS solution for all experiments was comprised of a mixture of 75% PEG-g-PLL and 25% PDL (v/v), diluted to 10 µg/ml [47]. C2C12 myoblast cells were seeded onto the patterned surfaces at a density of 2500 cells/cm^2, and imaged shortly after seeding and after 18 h of growth in an incubator.

In images of stained cells we observed lamellopodia of the myoblasts aligning with areas of netrin-1 patterned at higher density. This was most evident on the sinusoidal gradients,

as multiple alternating bands of high and low density netrin-1 are present underneath a single cell, revealing selective outgrowth on higher netrin-1 densities (Figures 3.5(d) and S3.5, white arrows). Localized pattern distortions were present in some of the fixed samples (Figure 3.5(c), white arrow, and Figure S3.5, blue arrow). While these distortions could be artifacts from the fixing process, it may be possible to extract traction forces from live cells patterned on these gradients by tracking the displacement of the nanodots [155].

To quantify the response of C2C12 cells to netrin-1 DNGs, cell positions were recorded on the gradients, and the data for all gradients with increasing density slopes were merged and used for analysis (control squares 21-34 in Figure S3.2 were excluded). Axes were defined for the gradients such that the density gradient extended in the x-direction, while the y-direction was perpendicular to the gradient profile. Control gradients of IgG (a neutral cue) were patterned and quantified as well. The cells were evenly distributed across the gradients after 18 h on the IgG gradients (Figure 3.6(a)), and at the start of the experiments on the netrin-1 gradients (Figure 3.6(b)), with a population mean at the center of the gradients ($x = 200$ µm) in each of these respective cases ($p = 0.6857$, $n = 4$ experiments; $p = 0.9407$, $n = 3$ experiments). Control squares of netrin-1 (i.e. gradients with zero slope) also showed an even distribution of cells after 18 h (data not shown). On the remainder of the netrin-1 gradients, the population mean shifted up the gradient over the course of 18 h ($p < 0.001$, $n = 5$ experiments). This shift is indicative of a haptotactic migratory response to the patterned netrin-1 gradients (Figure 3.6(c)). This shift may be seen clearly in box plots of the population distributions along the length of the gradients for each case (Figure 3.6(d)). Cell distribution in the y direction serves as an internal control for each case, as this direction is perpendicular to the direction of the gradient, and cells were found to be evenly distributed in all cases (Figure 3.6(e)). Cumulative distribution charts reveal that 54% of cells are in the lower density half of the gradients on IgG gradients, while on netrin-1 gradients, this value is 49% at the start of the experiment, and reduces to 35% over 18 h (Figure 3.6(f)). A perfectly evenly distributed cell population would have 50% of the cells in the lower half of the gradient, and 50% in the upper half.

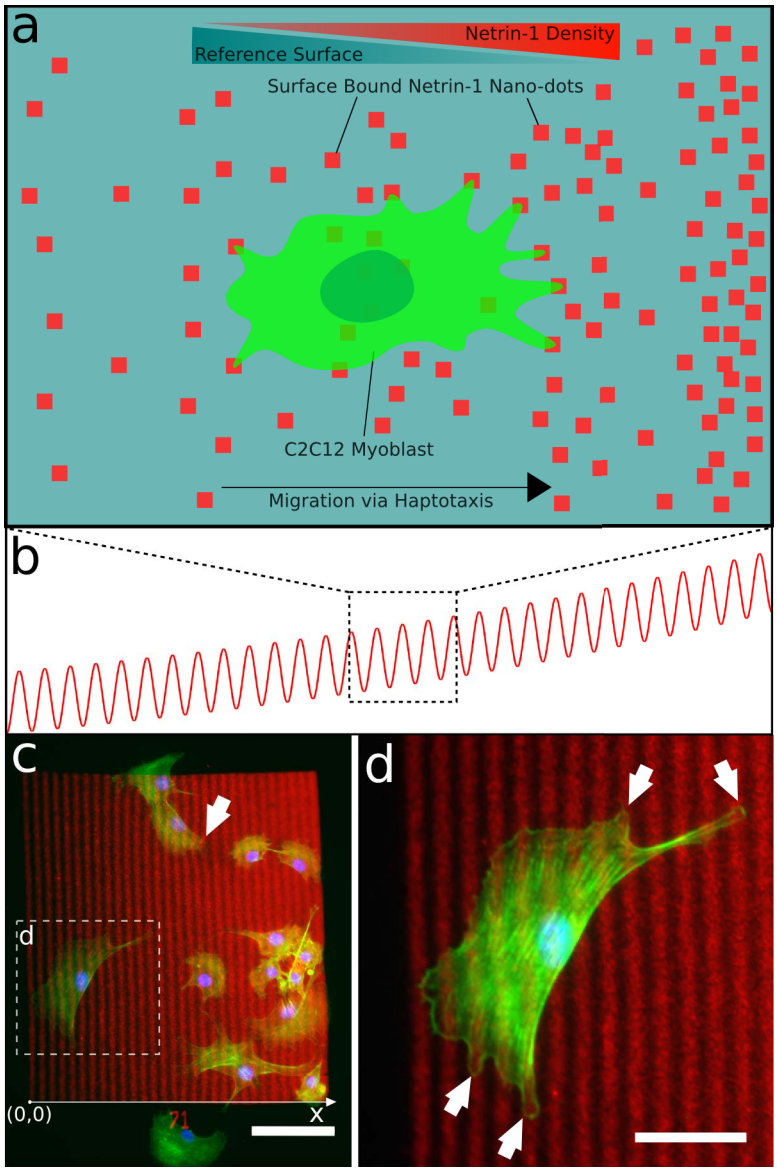
a
Netrin-1 Density
Reference Surface
Surface Bound Netrin-1 Nano-dots
C2C12 Myoblast
Migration via Haptotaxis
b
c
d
(0,0)
x
71

Figure 3.5

Figure 3.5: Haptotaxis assay: C2C12 cells on netrin-1 DNG patterned on Sylgard 527. a) Depiction of C2C12 myoblast on a netrin-1 DNG consisting of an exponentially increasing density profile with localized sinusoidal perturbations. b) The density profile for the gradient shown in this figure (#71 in Figure S3.2). This gradient features an exponential density profile with a dynamic range of 3.35 OM, up to 44.44% surface coverage at the high density end. A superimposed sinusoid introduces local oscillations of 7.5% density coverage with a period of 13.3 µm. The resultant high density bands of protein result in striking lamellopodia outgrowth patterns. c) Cells accumulate at higher densities of patterned netrin-1. The bottom left corner of the gradient is set as origin, and the x-axis extends up the gradient. The arrow denotes a region where local pattern deformation is visible, possibly due to traction forces on the substrate. d) Enlargement of inset in c). Arrows denote areas of the cell lamellopodia aligned with higher density bands of netrin-1. Scale bars are 100 µm in (c) and 50 µm in (d).

It should be noted that some of the cells at the high end of the gradients entered the gradient from surrounding areas, rather than migrating up the gradient. However, this is as likely to happen at the low density region of the gradient, and thus there is a clear preference for the high density areas of patterned netrin-1. To determine quantitative migration parameters, it would be necessary to correct for the arrival of cells from outside of the gradient. This could be done by tracing each cell with live imaging, but is beyond the scope of this work.

3.3.5 C2C12 Phenotype Changes in Response to High Netrin-1 Density

In addition to the shift in cell population distribution, C2C12 cell phenotypes were observed to change along the gradients of increasing netrin-1 density. Cells near the top of the gradients were larger and less circular, while cells at lower netrin-1 densities were often balled up and retracted (Figure 3.7(a)). This effect was most prominent on smoother gradients with larger dynamic ranges. To quantify the changes, cell area and circularity were measured on four of the smoothest gradients with the largest dynamic ranges (Figure 3.7(b-c)). It is noteworthy that this phenotypical change did not apply to all cells, as some smaller and more circular cells were present even at high netrin-1 densities, possibly due to the cell state

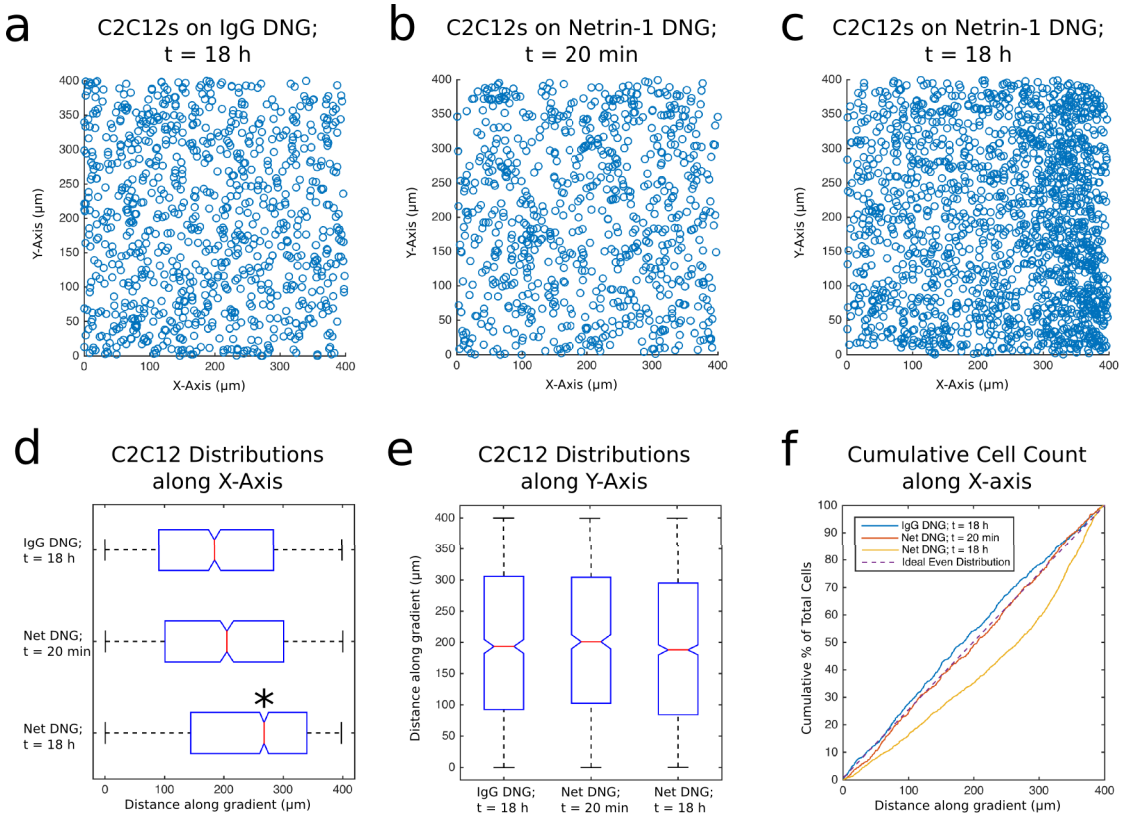

Figure 3.6: Analysis of cell positions on netrin-1 gradients patterned on Sylgard 527. Data was merged for all gradients of the gradient array (#1-20 and #35-100), while control squares (#21-34) were not considered (see Figure S3.2). Scatter plots show individual cell positions on the gradients after a) 18 h on an IgG gradient, b) 20 min on a netrin-1 gradient, and c) 18 h on a netrin-1 gradient. (d-e) Box plots of the cell distributions along the x- and y- axes for each case. The x-axis extends in the direction of the gradient, while the y-axis is perpendicular to the gradient. f) Cumulative cell count along the gradients for each data set in (a-c). A perfectly even distribution is depicted as a dashed line, which is closely matched by final cell distributions on IgG gradients and initial distributions on netrin-1 gradients. The population shift towards higher netrin-1 densities over 18 h manifests as a skewing of the cumulative cell count. *denotes shift from an expected mean of $x = 200$ μm with $p < 0.001$ ($n = 5$ experiments)

and cycle. Increased cell area and cell spreading is indicative of stronger adhesion to the substrate, and suggests that C2C12 cells adhere more strongly to substrates patterned with netrin-1 – an idea consistent with previously published results [46].

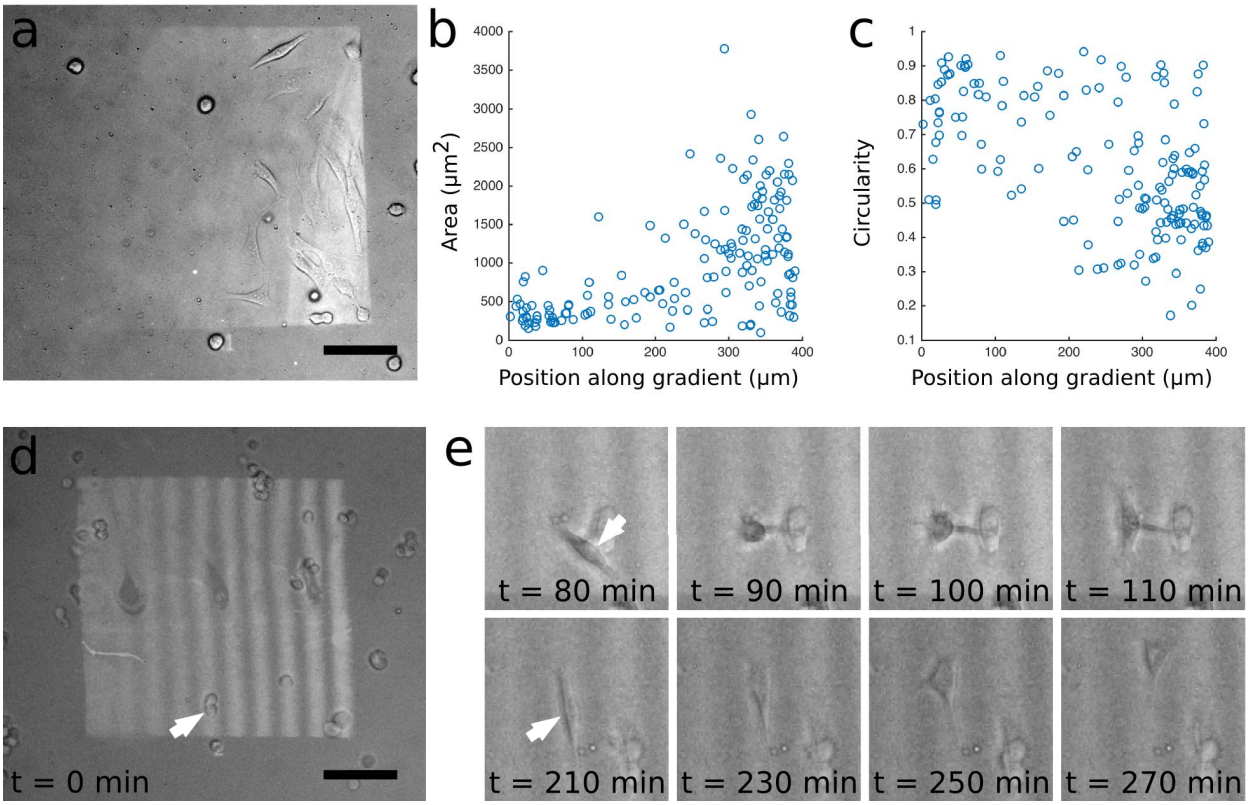

Figure 3.7: High density areas of netrin-1 prompt phenotypical changes to C2C12 cells. a) Cells at the high end of the gradients are more larger and less circular than cells elsewhere on the gradients or off the gradient. b) Quantification of cell area shows a clear increase following netrin-1 density analyzed on 400 μm long linear gradients ranging from 0.02% to 44.44% of surface coverage. c) Cell circularity recorded from the same data set shows a decrease towards the high end of the gradient, reflecting the more elongated phenotype of cells seen in a). $n = 3$ experiments, 4 gradients. Scale bar is 100 μm. d) Fluorescence image overlaid with brightfield to show the initial cell positions and gradient in Video S1. e) Enlarged still images from Video S1, centred on the cell indicated by the arrow in d). Two different sequences show how this cell moves by filopodial extension and sensing, followed by rapid contraction of the trailing edge.

To observe these phenotypical changes in real time, live imaging experiments were performed with C2C12s on netrin-1 gradients. In these experiments, sinusoidal gradients were

imaged because the high density bands of netrin-1 allowed for easy visualization of cells spreading out on higher netrin-1 densities. It was observed that cells migrated more slowly and spread out more when in contact with higher netrin-1 densities (Video S1). This suggests that netrin-1 promotes substrate adhesion for C2C12 cells, thus directing cells towards and 'trapping' them on the bands of higher netrin-1 density. Indeed, in the videos could be seen moving along bands of netrin-1 and occasionally jumping across bands. Cell motility proceeded according to an 'inching' mechanism [156] – cells would stretch out either along the band or across a gap to a new band, after which they would rapidly contract by releasing one extremity, and form a rounded shape at the other extremity (Figure 3.7(d-e)). This results in sporadic movement of the cells, as relatively static periods are interspersed with rapid jumps to new locations. These observations indicate that different gradient patterns may be used to investigate different aspects of cell migration – for example, these sinusoidal gradients allow for visualization of cells jumping between high density bands of netrin-1, which may be used in the future to study the range of sensing by filopodial extensions.

3.4 Conclusions

To the best of our knowledge, this work represents the first time that bioactive protein gradients with nanometer sized features have been successfully patterned via lift-off nanocontact printing on soft substrates with stiffnesses < 10 kPa. We demonstrated that even brief exposure to plasma altered the mechanical properties of soft PDMS substrates, and therefore a patterning technique was developed that did not involve plasma activation of the final substrate. DNGs were patterned on PDMS substrates with physiological stiffness and the patterned gradients matched the original design with $< 5\%$ average skewing. Reference surface proteins were shown to adsorb to soft PDMS substrates as well as on glass substrates, without the need for plasma activation. Patterned DNGs of netrin-1 with a RS of 75% PEG-g-PLL and 25% PDL were shown to promote accumulation of C2C12 cells at higher netrin-1 densities over a period of 18 h. C2C12 cells were also found to become larger and

less circular on areas of higher netrin-1 density, indicating that netrin-1 promotes substrate adhesion in C2C12 myoblast cells.

The method developed here to pattern nanodots on soft surfaces will allow studying of cell migration in response to DNGs and other arbitrary patterns on substrates with physiological rigidity, and will allow comparison of the response to patterns on soft and hard substrates. Patterned soft substrates will be particularly useful to study the impact of substrate rigidity on the haptotaxis of primary cells, such as the extension of axons in neuronal cells that are known to respond to netrin-1 [157], as well as the migration of immune cells such as neutrophils [158, 159]. The effect that altering substrate stiffness has on initial neuronal outgrowth has been noted in the past [3, 4, 118], providing further motivation for protein patterning on soft substrates.

In the future, visualizing local deformations in ordered nanodot patterns, as observed here, could offer a new technique for measuring traction forces on soft substrates, based on prior knowledge of the dot placement. Additionally, live imaging of cell migration on DNGs could offer new insights into mechanisms of cellular motility, for example by observing how gaps between high density protein bands are navigated.

Acknowledgements

The authors would like to thank Dr. Sébastien Ricoult for his advice throughout this project and Abhishek Sinha for his help with cell culture and troubleshooting. Madeleine Anthonisen performed the AFM measurements, and a custom Matlab code written by Xue Ying Chua was used to extract the Young's modulus. We acknowledge financial support from NSERC. DM was supported by an NSERC CGSM and NSERC CREATEs. TEK was supported by an FRQS Chercheur Nationaux award and a Killam Foundation Scholar award. DJ was supported by a Canada Research Chair.

3.5 Supplementary Information

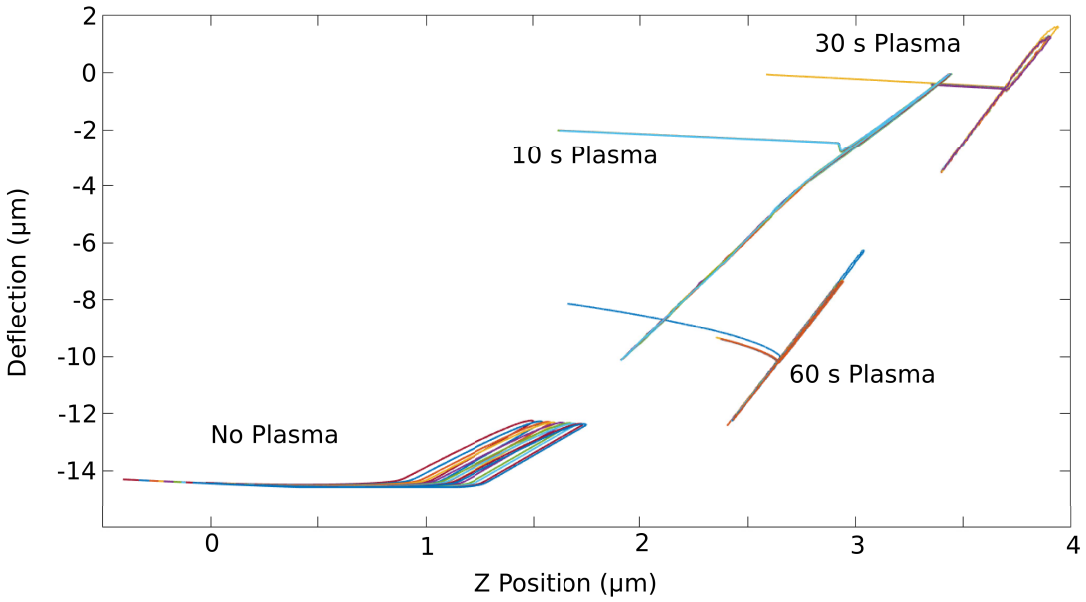

Figure S3.1: AFM indentation measurements. Curves show advancement and retraction of AFM cantilever at the surface of Sylgard 527 after 0-60 s of plasma activation. The Young's modulus of the interface may be extracted from the slope of the inbound deflection curve, with higher slopes indicative of increased deflection and thus a stiffer substrate [160].

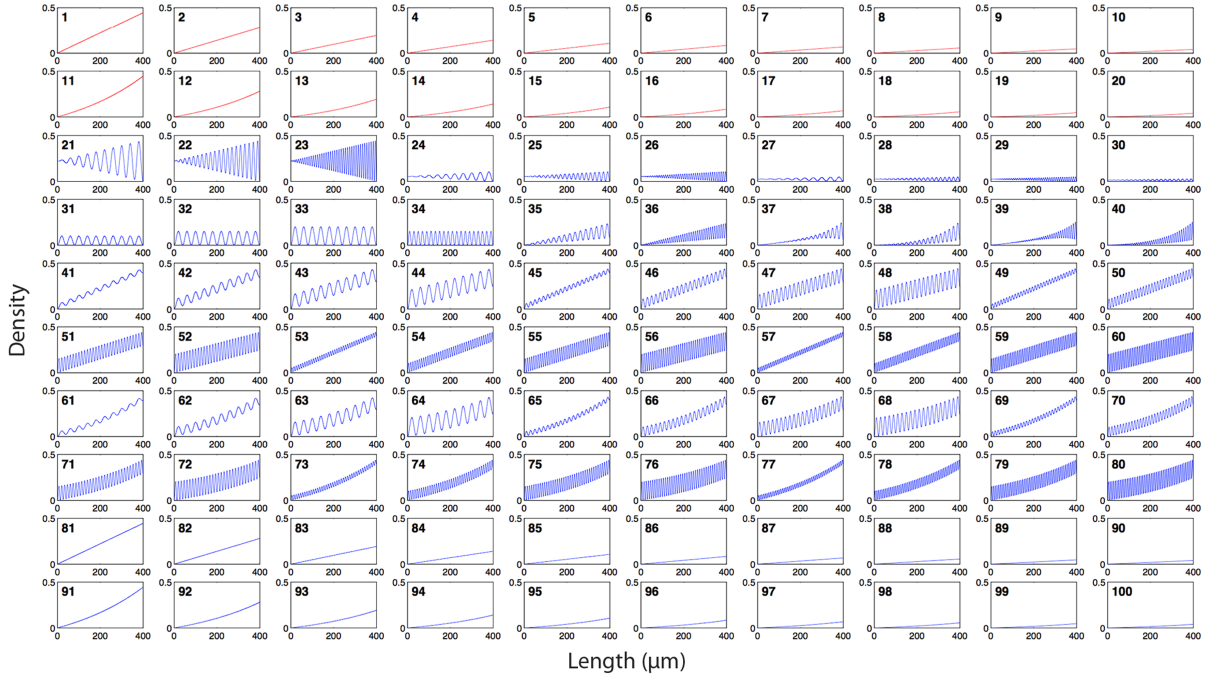

Figure S3.2: Each box shows the density function of one gradient. Gradients 1-20 are ordered gradients, with 1-10 having linear slopes, while 11-20 have exponential slopes. Gradients 81-100 are equivalent to 1-20, but with random dot placement, rather than ordered. Gradients 21-34 have sinusoidal density envelopes with no positive slope, and serve as control gradients – 21-30 have linearly increasing sinusoid amplitude, while 31-34 have constant amplitude. Gradients 35-36 have a linear slope superimposed on a sinusoid with linearly increasing amplitude, while 37-40 use an exponential slope on a sinusoid with exponentially increasing amplitude. Gradients 41-60 have a linear slope with a sinusoid of constant amplitude, while 61-80 have exponential slopes with sinusoids of constant amplitude. For a more detailed explanation of the gradient array, refer to Ongo *et al.* [79].

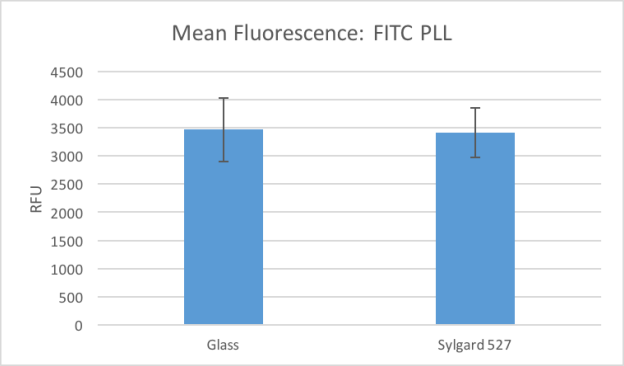

(a) FITC PLL coating on glass and Sylgard 527; 1 hour incubation; no plasma activation

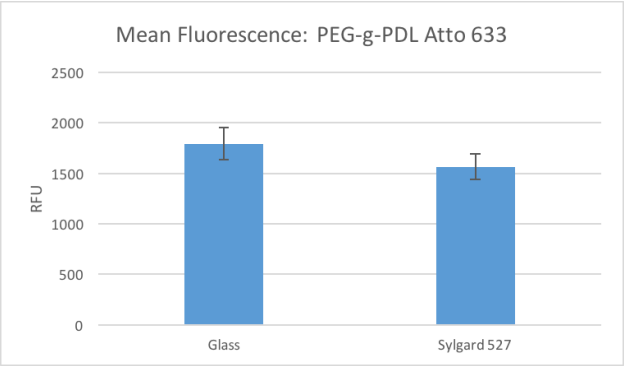

(b) Atto 633 PEG-g-PDL coating on glass and Sylgard 527; 1 hour incubation; no plasma activation

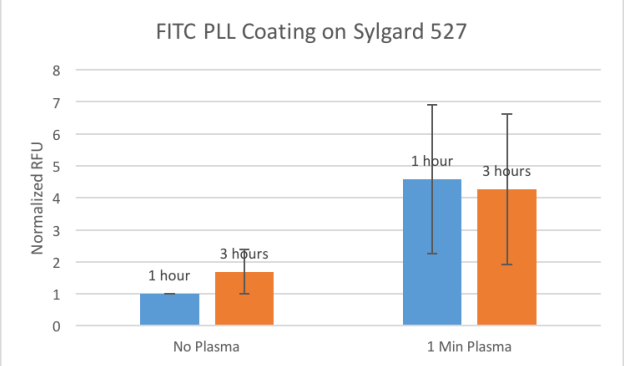

(c) FITC PLL coating on Sylgard 527; comparison of incubation time and plasma vs. no plasma

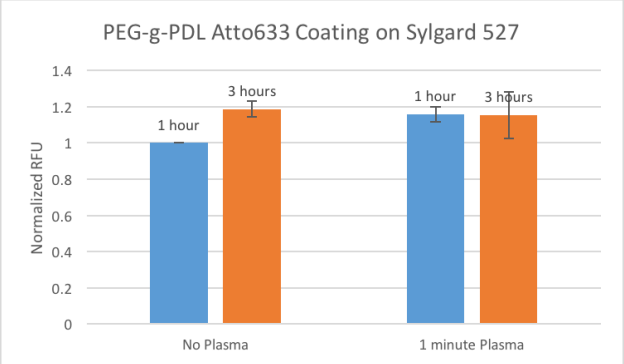

(d) Atto 633 PEG-g-PDL coating on Sylgard 527; comparison of incubation time and plasma vs. no plasma

Figure S3.3: Quantitative analysis of fluorescent reference surface coatings. Mean fluorescence levels of images such as those in Figure S3.4 were measured using ImageJ. Error bars denote standard error of the mean, based on 12-15 measurements for (a-b), and 4 measurements for (c-d).

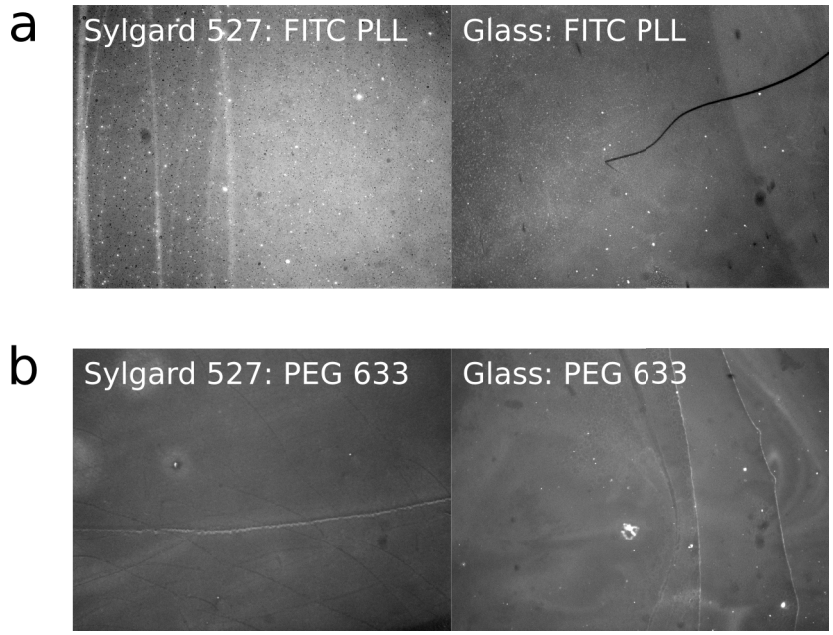

Figure S3.4: Typical fluorescent reference surface coatings. a) FITC tagged poly-L-lysine adsorption onto Sylgard 527 and glass, no plasma activation, incubation for 1 hour followed by rinsing with milliQ water. b) Atto 633 tagged PEG-g-PDL adsorbed onto Sylgard 527 and glass, no plasma activation, incubation for 1 hour followed by rinsing with milliQ water. Images are all adjusted to conform to the same LUT. Aberrations in the surfaces are attributed to surface deformities, and are observed to be equally present in coatings on both glass and Sylgard 527.

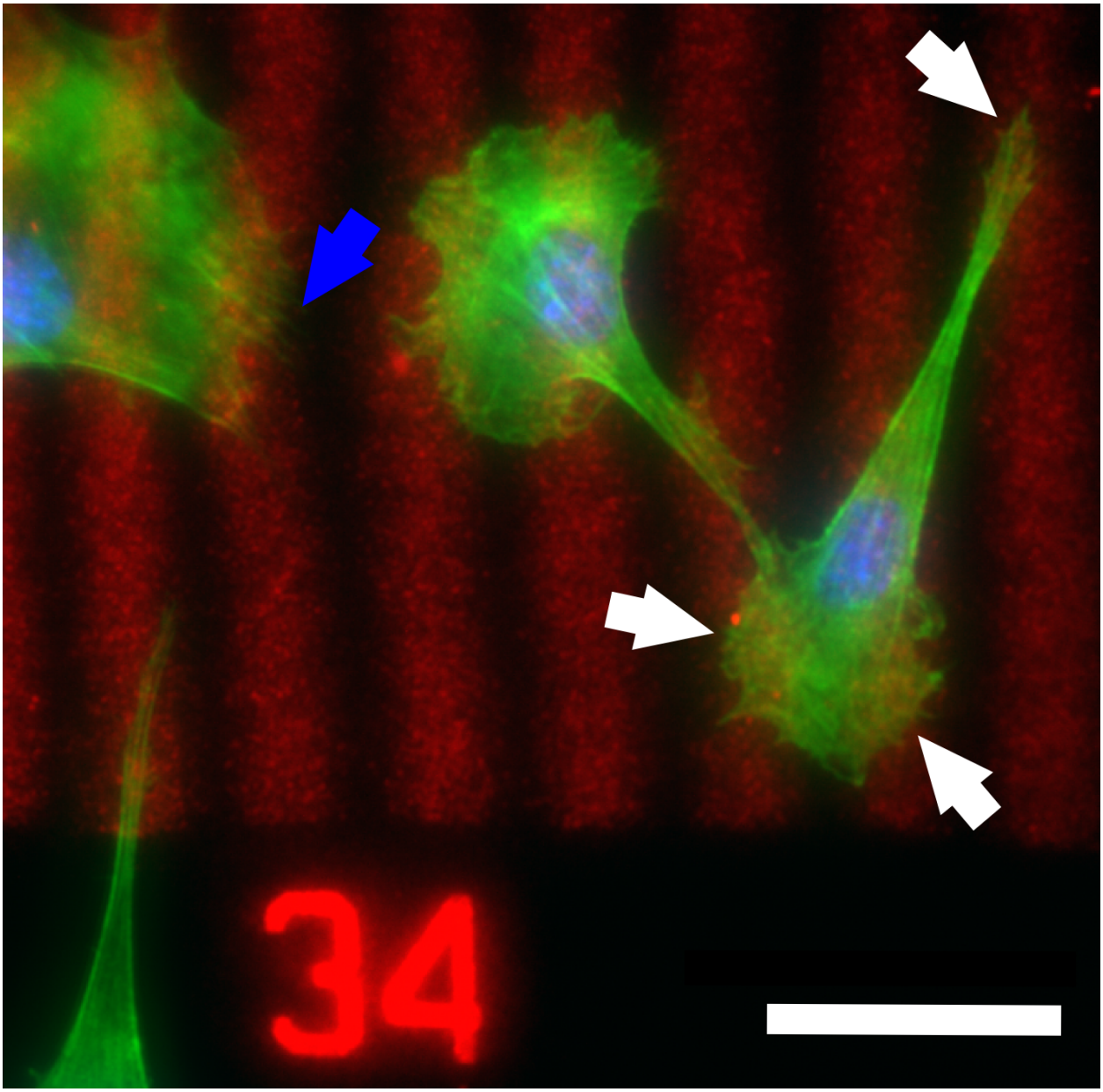

Figure S3.5: C2C12s on Netrin gradients on Sylgard 527: white arrows denote apparent adhesion of the cell lamellopodia to bands of high Netrin density, while the blue arrow indicates local deformation of the pattern on Sylgard 527. Deformations such as these may be used to measure cell traction forces in the future. Scale bar is 50 µm.

4 General Discussion

The manuscript presented in this thesis demonstrates the work performed on this project. For the purposes of this discussion section, the work will be divided into three main parts. First, a novel adaptation of microcontact printing was used to transfer protein patterns consisting of nanometer sized features onto the soft, tacky surface of Sylgard 527. Second, the adsorption of PLL and PEG-g-PLL to Sylgard 527 was demonstrated using fluorescence measurements, to illustrate that a backfilled reference surface could be applied to Sylgard 527. Finally, C2C12 cells were seeded on patterned gradients of netrin-1, and their response to the gradients were observed. In addition to that offered in the manuscript, some discussion points concerning each of these areas of work are presented below.

4.0.1 Patterning of Nanodots on Sylgard 527: Pattern Fidelity and Skewing

Patterns consisting of 200×200 nm^2 dots were transferred successfully to Sylgard 527 using lift-off microcontact printing on a dissolvable intermediate film of PVA. This process eliminated the need to plasma activate the Sylgard 527 to achieve protein transfer from the stamp to the final substrate, a step which is usually necessary in traditional microcontact printing. This elimination of plasma treatment was crucial, as our tests indicate that plasma activation changes the mechanical properties of the Sylgard 527 by forming a thin layer of glass on the surface of the material. In general, the fidelity of the patterns was very good, however it should be mentioned that a certain amount of practice was required to become comfortable with the process and to achieve a high success rate with the prints. As with patterning on glass, a number of prints fail to transfer properly, even when the process is performed by practiced hands. While we did not perform any quantitative analysis of this, observationally it may be said that the failure rate was approximately equal between patterning on glass and patterning on Sylgard 527. In fact, because of the tackiness of Sylgard 527, good contact between the flexible PVA film and the surface of the Sylgard 527 is almost guaranteed, contributing to the success rate of these prints.

That being said, printing on Sylgard 527 suffers from another disadvantage which is difficult to control. While transfer of the pattern worked almost every time, the way in which the PVA film was laid on the surface of the Sylgard 527 affected the skewing of the pattern. It was quite common that, even though the patterns transferred, the gradients were very skewed, to the point of not being useable. Again, no quantitative analysis of this was performed – largely skewed patterns were simply discarded. Even when the patterns appeared to be perfect, overlaying high magnification images of the gradients onto the same gradients printed on glass revealed that a small degree of skewing was present in every print. This skewing may be the largest limitation of the proposed technique. To address this issue, it is recommended that a system could be developed to enable hands free contact between the PVA film and the Sylgard 527. This could be a simple hinged lever device, which contacts the two substrates in a controllable and repeatable way for each print, and such a device would add a large degree of utility and reliability to the patterning technique shown here.

4.0.2 Characterization of Reference Surfaces on Sylgard 527

Previous papers which coat PDMS with cell adhesion promoting molecules, such as collagen or fibronectin, commonly plasma activate the PDMS before applying the coating [7, 121]. As mentioned before, plasma treatment of Sylgard 527 alters the mechanical properties of the material, and is not a viable option for the types of experiments performed in this work. By coating Sylgard 527 with fluorescently tagged versions of PLL and PEG-g-PLL, it was determined that the reference surface was coating the PDMS surface approximately the same as it coated a glass surface, without the need for plasma activation. However, there was a high degree of variation between samples, resulting in large standard deviations in each case. Thus, it is not clear exactly how repeatable these measurements are, and a more rigorous characterization of the adsorption of reference surface to the Sylgard 527 would serve to strengthen the data presented in this work. For example, functional studies of cell response to a stripe assay with different reference surface coatings would provide a more convincing

case that the reference surface coating is functioning as desired on Sylgard 527.

4.0.3 Migratory Response to Patterned Netrin-1 Nanodot Gradients

When C2C12 myoblast cells were cultured on the patterned netrin-1 gradients, a shift in average cell distribution was observed over time, with cells accumulating at the higher density end of the gradients. While the general shift in distribution is fairly clear, it should be noted that this is the average cell distribution over an array of different gradients. While the density of all gradients used increases along the length of the gradient, it does so with different density profiles for each gradient (the array of gradients consists of 100 different gradient profiles) [79]. Thus, while a general migratory trend is observed, it is possible that this trend is stronger on some gradient profiles than on others. While a large number of cells were analyzed, the cells on each individual gradient were not that many, and thus it was decided that the results should be averaged across each of the different gradients to increase the statistical power of our observations. However, it is our belief that more observations may be made about specific gradient slopes and shapes if the amount of data for each gradient in the array is increased sufficiently.

5 Conclusions

5.1 Project Summary

In this work, a novel technique for patterning nanometer sized spots of protein on soft substrates was demonstrated. This technique was used to pattern digital nanodot gradients on Sylgard 527, a form of PDMS with an elastic modulus close to that of brain tissue (< 10 kPa). We demonstrated that even brief exposure to plasma altered the mechanical properties of soft PDMS substrates, and therefore a patterning technique was developed that did not involve plasma activation of the final substrate. DNGs were patterned on Sylgard 527

such that the patterned gradients matched the original design with $< 5\%$ average skewing. Reference surface proteins were shown to adsorb to soft PDMS substrates as well as on glass substrates, without the need for plasma activation. Patterned DNGs of netrin-1 with a RS of 75% PEG-g-PLL and 25% PDL were shown to promote accumulation of C2C12 cells at higher netrin-1 densities over a period of 18 h. C2C12 cells were also found to become larger and less circular on areas of higher netrin-1 density, indicating that netrin-1 promotes substrate adhesion in C2C12 myoblast cells. To the best of our knowledge, this work represents the first time that protein patterns with feature sizes in the nanometer range have been successfully patterned via lift-off nanocontact printing on soft, tacky substrates with stiffnesses < 10 kPa. As well, this is the first study which demonstrates a haptotaxis migration assay on an soft substrate. This technique is proposed as a platform technology which could be used to investigate the effect that substrate stiffness has on cellular migration via surface bound protein gradients.

5.2 Suggestions for Future Work

5.2.1 Investigation of Haptotaxis with Substrate Stiffness Modulation

One of the intentions of this assay is to use it to investigate whether the stiffness of the underlying substrate will impact cellular migration via substrate bound cues. Based on observations that the substrate stiffness affects other aspects of cellular motility, from focal adhesion formation to cytoskeletal rearrangement observed in durotaxis, it is clear that cells can transduce information about the stiffness of their environment through intracellular signalling pathways. Whether this transduction into downstream signalling pathways has any effect on the mechanotransduction of substrate bound chemical cues during haptotaxis remains to be seen, but it is an interesting biological question that could be properly investigated using the technology presented here, and comparing cellular responses to the gradients between soft and hard substrates.

5.2.2 Using Nanopatterned Proteins to Measure Cellular Traction Forces on Soft Substrates

The observation that localized distortions of the protein patterns were present around certain cells prompted the idea that this technique would also be adapted to measure the traction forces of live cells on soft substrates. Initial experiments with live cells have been promising, as local pattern deformations are indeed visible around the cellular membrane. We postulate that, using prior knowledge of the pattern design and the modulus of the material, local distortions may be measured and used to extract the traction forces present at the surface.

An important point to consider in this regard is that traction force measurements are typically made based on the assumption that surface deflections due to traction forces are made in plane. This assumption will need to be carefully validated if the observed deformations of Sylgard 527 are to be used in future traction force measurements.

5.2.3 Application to Neuroscience: Axon Guidance Assays

A major perceived application of the assay developed in this work is in the field of neuroscience. Axon guidance studies are often performed on glass substrates. It has been demonstrated that axons extend faster and develop more complex branches on softer substrates with stiffnesses in the range of brain tissue. It would be of interest to see if the process of axon guidance is also affected by the substrate stiffness. The work shown here utilised netrin-1 as a patterned protein because it is an axon guidance cue, and it was the intention to demonstrate the utility of this assay with an axon guidance cue such that it might be extended into the field of neuroscience in the future.

References

[1] Ricoult, S.G. *et al.* Large dynamic range digital nanodot gradients of biomolecules made by low-cost nanocontact printing for cell haptotaxis. *Small* 9, 3308–3313 (2013).

[2] Geiger, B., Spatz, J.P., & Bershadsky, A.D. Environmental sensing through focal adhesions. *Nature Reviews Molecular Cell Biology* 10, 21–33 (2009).

[3] Balgude, A.P., Yu, X., Szymanski, A., & Bellamkonda, R.V. Agarose gel stiffness determines rate of DRG neurite extension in 3d cultures. *Biomaterials* 22, 1077–1084 (2001).

[4] Flanagan, L.A., Ju, Y.E., Marg, B., Osterfield, M., & Janmey, P.A. Neurite branching on deformable substrates. *Neuroreport* 13, 2411–2415 (2002).

[5] Madsen, E.L. *et al.* Instrument for determining the complex shear modulus of soft-tissue-like materials from 10 to 300 Hz. *Physics in medicine and biology* 53, 5313–5342 (2008).

[6] Yu, H., Xiong, S., Tay, C.Y., Leong, W.S., & Tan, L.P. A novel and simple microcontact printing technique for tacky, soft substrates and/or complex surfaces in soft tissue engineering. *Acta Biomaterialia* 8, 1267–1272 (2012).

[7] Natarajan, V., Berglund, E.J., Chen, D.X., & Kidambi, S. Substrate stiffness regulates primary hepatocyte functions. *RSC Advances* 5, 80956–80966 (2015).

[8] Palchesko, R.N., Lathrop, K.L., Funderburgh, J.L., & Feinberg, A.W. In vitro expansion of corneal endothelial cells on biomimetic substrates. *Scientific Reports* 5, 7955 (2015).

[9] Palchesko, R.N., Zhang, L., Sun, Y., & Feinberg, A.W. Development of polydimethylsiloxane substrates with tunable elastic modulus to study cell mechanobiology in muscle and nerve. *PLOS ONE* 7, e51499 (2012).

[10] Caballero, D., Comelles, J., Piel, M., Voituriez, R., & Riveline, D. Ratchetaxis: long-range directed cell migration by local cues. *Trends in Cell Biology* 25, 815–827 (2015).

[11] Reig, G., Pulgar, E., & Concha, M.L. Cell migration: from tissue culture to embryos. *Development* 141, 1999–2013 (2014).

[12] Shellard, A. & Mayor, R. Chemotaxis during neural crest migration. *Seminars in Cell & Developmental Biology* (2016).

[13] Goodhill, G.J. Can molecular gradients wire the brain? *Trends in Neurosciences* (2016).

[14] Delgado, I. & Torres, M. Gradients, waves and timers, an overview of limb patterning models. *Seminars in Cell & Developmental Biology* 49, 109–115 (2016).

[15] Briscoe, J. & Small, S. Morphogen rules: design principles of gradient-mediated embryo patterning. *Development* 142, 3996–4009 (2015).

[16] Lander, A.D., Nie, Q., & Wan, F.Y.M. Do morphogen gradients arise by diffusion? *Developmental Cell* 2, 785–796 (2002).

[17] Yu, S.R. *et al.* Fgf8 morphogen gradient forms by a source-sink mechanism with freely diffusing molecules. *Nature* 461, 533–536 (2009).

[18] Browne, L.H. & Williams, K.L. Gradients in the expression of cell surface glycoproteins in a simple tissue, the Dictyostelium discoideum slug. *Microbiology* 139, 847–853 (1993).

[19] Gurdon, J.B. & Bourillot, P.Y. Morphogen gradient interpretation. *Nature* 413, 797–803 (2001).

[20] Aznavoorian, S., Stracke, M.L., Krutzsch, H., Schiffmann, E., & Liotta, L.A. Signal transduction for chemotaxis and haptotaxis by matrix molecules in tumor cells. *The Journal of Cell Biology* 110, 1427–1438 (1990).

[21] Van Haastert, P.J.M. & Devreotes, P.N. Chemotaxis: signalling the way forward. *Nature Reviews Molecular Cell Biology* 5, 626–634 (2004).

[22] Vladimirov, N. & Sourjik, V. Chemotaxis: how bacteria use memory. *Biological Chemistry* 390, 1097–1104 (2009).

[23] Roussos, E.T., Condeelis, J.S., & Patsialou, A. Chemotaxis in cancer. *Nature Reviews Cancer* 11, 573–587 (2011).

[24] Carter, S.B. Principles of cell motility: the direction of cell movement and cancer invasion. *Nature* 208, 1183–1187 (1965).

[25] Taraboletti, G., Roberts, D.D., & Liotta, L.A. Thrombospondin-induced tumor cell migration: haptotaxis and chemotaxis are mediated by different molecular domains. *The Journal of Cell Biology* 105, 2409–2415 (1987).

[26] Keller, H.U., Wissler, J.H., & Ploem, J. Chemotaxis is not a special case of haptotaxis. *Experientia* 35, 1669–1671 (1979).

[27] Ricoult, S.G., Kennedy, T.E., & Juncker, D. Substrate-bound protein gradients to study haptotaxis. *Biomaterials* 3, 40 (2015).

[28] Wong, K., Park, H.T., Wu, J.Y., & Rao, Y. Slit proteins: molecular guidance cues for cells ranging from neurons to leukocytes. *Current Opinion in Genetics & Development* 12, 583–591 (2002).

[29] O'Donnell, M., Chance, R.K., & Bashaw, G.J. Axon growth and guidance: receptor regulation and signal transduction. *Annual Review of Neuroscience* 32, 383–412 (2009).

[30] Guan, K.L. & Rao, Y. Signalling mechanisms mediating neuronal responses to guidance cues. *Nature Reviews Neuroscience* 4, 941–956 (2003).

[31] Chilton, J.K. Molecular mechanisms of axon guidance. *Developmental Biology* 292, 13–24 (2006).

[32] Van Battum, E.Y., Brignani, S., & Pasterkamp, R.J. Axon guidance proteins in neurological disorders. *The Lancet Neurology* 14, 532–546 (2015).

[33] Baier, H. & Bonhoeffer, F. Axon guidance by gradients of a target-derived component. *Science* 255, 472–475 (1992).

[34] Tessier-Lavigne, M. Down the slippery slope. *Current Biology* 2, 353–355 (1992).

[35] McLaughlin, T. & O'Leary, D.D.M. Molecular gradients and development of retinotopic maps. *Annual Review of Neuroscience* 28, 327–355 (2005).

[36] Baker, K.A., Moore, S.W., Jarjour, A.A., & Kennedy, T.E. When a diffusible axon guidance cue stops diffusing: roles for netrins in adhesion and morphogenesis. *Current Opinion in Neurobiology* 16, 529–534 (2006).

[37] Deiner, M.S. *et al.* Netrin-1 and DCC mediate axon guidance locally at the optic disc: loss of function leads to optic nerve hypoplasia. *Neuron* 19, 575–589 (1997).

[38] Brankatschk, M. & Dickson, B.J. Netrins guide Drosophila commissural axons at short range. *Nature Neuroscience* 9, 188–194 (2006).

[39] Kennedy, T.E., Serafini, T., de la Torre, J., & Tessier-Lavigne, M. Netrins are diffusible chemotropic factors for commissural axons in the embryonic spinal cord. *Cell* 78, 425–435 (1994).

[40] Kennedy, T.E., Wang, H., Marshall, W., & Tessier-Lavigne, M. Axon guidance by diffusible chemoattractants: a gradient of netrin protein in the developing spinal cord. *The Journal of Neuroscience* 26, 8866–8874 (2006).

[41] Manitt, C. & Kennedy, T.E. Where the rubber meets the road: netrin expression and function in developing and adult nervous systems. In *Progress in Brain Research*, 425–442. Elsevier (2002).

[42] Grandin, M. *et al.* Structural decoding of the netrin-1/unc5 interaction and its therapeutical implications in cancers. *Cancer Cell* 29, 173–185 (2016).

[43] Keino-Masu, K. *et al.* Deleted in colorectal cancer (DCC) encodes a netrin receptor. *Cell* 87, 175–185 (1996).

[44] Wang, H., Copeland, N.G., Gilbert, D.J., Jenkins, N.A., & Tessier-Lavigne, M. Netrin-3, a mouse homolog of human NTN2l, is highly expressed in sensory ganglia and shows differential binding to netrin receptors. *The Journal of Neuroscience: The Official Journal of the Society for Neuroscience* 19, 4938–4947 (1999).

[45] Kang, J.S. *et al.* Netrins and neogenin promote myotube formation. *The Journal of Cell Biology* 167, 493–504 (2004).

[46] Srinivasan, K., Strickland, P., Valdes, A., Shin, G.C., & Hinck, L. Netrin-1/neogenin interaction stabilizes multipotent progenitor cap cells during mammary gland morphogenesis. *Developmental Cell* 4, 371–382 (2003).

[47] Ricoult, S.G., Thompson-Steckel, G., Correia, J.P., Kennedy, T.E., & Juncker, D. Tuning cell–surface affinity to direct cell specific responses to patterned proteins. *Biomaterials* 35, 727–736 (2014).

[48] Walter, J., Kern-Veits, B., Huf, J., Stolze, B., & Bonhoeffer, F. Recognition of position-specific properties of tectal cell membranes by retinal axons in vitro. *Development* 101, 685–696 (1987).

[49] Knöll, B., Weinl, C., Nordheim, A., & Bonhoeffer, F. Stripe assay to examine axonal guidance and cell migration. *Nature Protocols* 2, 1216–1224 (2007).

[50] Poliak, S. *et al.* Synergistic integration of Netrin and ephrin axon guidance signals by spinal motor neurons. *eLife* 4, e10841 (2015).

[51] Nichol, R.H., Hagen, K.M., Lumbard, D.C., Dent, E.W., & Gómez, T.M. Guidance of axons by local coupling of retrograde flow to point contact adhesions. *The Journal of Neuroscience* 36, 2267–2282 (2016).

[52] Jeon, N.L. *et al.* Generation of solution and surface gradients using microfluidic systems. *Langmuir* 16, 8311–8316 (2000).

[53] Caelen, I. *et al.* Formation of gradients of proteins on surfaces with microfluidic networks. *Langmuir* 16, 9125–9130 (2000).

[54] Smith, J.T. *et al.* Measurement of cell migration on surface-bound fibronectin gradients. *Langmuir* 20, 8279–8286 (2004).

[55] Juncker, D., Schmid, H., & Delamarche, E. Multipurpose microfluidic probe. *Nature Materials* 4, 622–628 (2005).

[56] Mai, J., Fok, L., Gao, H., Zhang, X., & Poo, M.m. Axon initiation and growth cone turning on bound protein gradients. *The Journal of Neuroscience* 29, 7450–7458 (2009).

[57] Bélisle, J.M., Correia, J.P., Wiseman, P.W., Kennedy, T.E., & Costantino, S. Patterning protein concentration using laser-assisted adsorption by photobleaching, LAPAP. *Lab on a Chip* 8, 2164 (2008).

[58] Bélisle, J.M., Kunik, D., & Costantino, S. Rapid multicomponent optical protein patterning. *Lab on a Chip* 9, 3580 (2009).

[59] von Philipsborn, A.C. *et al.* Microcontact printing of axon guidance molecules for generation of graded patterns. *Nature Protocols* 1, 1322–1328 (2006).

[60] Philipsborn, A.C.v. *et al.* Growth cone navigation in substrate-bound ephrin gradients. *Development* 133, 2487–2495 (2006).

[61] Coyer, S.R., García, A.J., & Delamarche, E. Facile preparation of complex protein architectures with sub-100-nm resolution on surfaces. *Angewandte Chemie International Edition* 46, 6837–6840 (2007).

[62] Trappmann, B. *et al.* Extracellular-matrix tethering regulates stem-cell fate. *Nature Materials* 11, 642–649 (2012).

[63] Wilbur, J.L., Kumar, A., Kim, E., & Whitesides, G.M. Microfabrication by microcontact printing of self-assembled monolayers. *Advanced Materials* 6, 600–604 (1994).

[64] Folkers, J.P., Laibinis, P.E., & Whitesides, G.M. Self-assembled monolayers of alkanethiols on gold: comparisons of monolayers containing mixtures of short- and long-chain constituents with methyl and hydroxymethyl terminal groups. *Langmuir* 8, 1330–1341 (1992).

[65] Folkers, J.P., Laibinis, P.E., & Whitesides, G.M. Self-assembled monolayers of alkanethiols on gold: the adsorption and wetting properties of monolayers derived from two components with alkane chains of different lengths. *Journal of Adhesion Science and Technology* 6, 1397–1410 (1992).

[66] Bernard, A. *et al.* Printing patterns of proteins. *Langmuir* 14, 2225–2229 (1998).

[67] Shen, K., Qi, J., & Kam, L.C. Microcontact printing of proteins for cell biology. *Journal of Visualized Experiments : JoVE* (2008).

[68] Ruiz, S.A. & Chen, C.S. Microcontact printing: A tool to pattern. *Soft Matter* 3, 168–177 (2007).

[69] Kaufmann, T. & Ravoo, B.J. Stamps, inks and substrates: polymers in microcontact printing. *Polymer Chemistry* 1, 371–387 (2010).

[70] Xia, Y. & Whitesides, a.G.M. Soft lithography. *Annual Review of Materials Science* 28, 153–184 (1998).

[71] Weibel, D.B. *et al.* Bacterial printing press that regenerates its ink: contact-printing bacteria using hydrogel stamps. *Langmuir* 21, 6436–6442 (2005).

[72] Choi, M.K. *et al.* Wearable red-green-blue quantum dot light-emitting diode array using high-resolution intaglio transfer printing. *Nature Communications* 6, 7149 (2015).

[73] Ricoult, S.G., Goldman, J.S., Stellwagen, D., Juncker, D., & Kennedy, T.E. Generation of microisland cultures using microcontact printing to pattern protein substrates. *Journal of Neuroscience Methods* 208, 10–17 (2012).

[74] Qin, D., Xia, Y., & Whitesides, G.M. Soft lithography for micro- and nanoscale patterning. *Nature Protocols* 5, 491–502 (2010).

[75] Renault, J.P. *et al.* Fabricating arrays of single protein molecules on glass using microcontact printing. *The Journal of Physical Chemistry B* 107, 703–711 (2003).

[76] Hlady, V. & Buijs, J. Protein adsorption on solid surfaces. *Current Opinion in Biotechnology* 7, 72–77 (1996).

[77] Rabe, M., Verdes, D., & Seeger, S. Understanding protein adsorption phenomena at solid surfaces. *Advances in Colloid and Interface Science* 162, 87–106 (2011).

[78] Ricoult, S.G., Nezhad, A.S., Knapp-Mohammady, M., Kennedy, T.E., & Juncker, D. Humidified microcontact printing of proteins: universal patterning of proteins on both low and high energy surfaces. *Langmuir: the ACS journal of surfaces and colloids* 30, 12002–12010 (2014).

[79] Ongo, G., Ricoult, S.G., Kennedy, T.E., & Juncker, D. Ordered, random, monotonic and non-monotonic digital nanodot gradients. *PloS One* 9, e106541 (2014).

[80] Wadu-Mesthrige, K., Xu, S., Amro, N.A., & Liu, G.y. Fabrication and imaging of nanometer-sized protein patterns. *Langmuir* 15, 8580–8583 (1999).

[81] Li, Y., Maynor, B.W., & Liu, J. Electrochemical AFM "dip-pen" nanolithography. *Journal of the American Chemical Society* 123, 2105–2106 (2001).

[82] Salaita, K. *et al.* Sub-100 nm, centimeter-scale, parallel dip-pen nanolithography. *Small* 1, 940–945 (2005).

[83] Harnett, C.K., Satyalakshmi, K.M., & Craighead, H.G. Bioactive templates fabricated by low-energy electron beam lithography of self-assembled monolayers. *Langmuir* 17, 178–182 (2001).

[84] Taha, H. *et al.* Protein printing with an atomic force sensing nanofountainpen. *Applied Physics Letters* 83, 1041–1043 (2003).

[85] Leipzig, N.D. & Shoichet, M.S. The effect of substrate stiffness on adult neural stem cell behavior. *Biomaterials* 30, 6867–6878 (2009).

[86] Park, J.S. *et al.* The effect of matrix stiffness on the differentiation of mesenchymal stem cells in response to TGF-β. *Biomaterials* 32, 3921–3930 (2011).

[87] Engler, A.J., Sen, S., Sweeney, H.L., & Discher, D.E. Matrix elasticity directs stem cell lineage specification. *Cell* 126, 677–689 (2006).

[88] Huebsch, N. *et al.* Matrix elasticity of void-forming hydrogels controls transplanted-stem-cell-mediated bone formation. *Nature Materials* 14, 1269–1277 (2015).

[89] Discher, D.E., Janmey, P., & Wang, Y.l. Tissue cells feel and respond to the stiffness of their substrate. *Science* 310, 1139–1143 (2005).

[90] Steinberg, M.S. Mechanism of tissue reconstruction by dissociated cells. II. Time-course of events. *Science* 137, 762–763 (1962).

[91] Hiramatsu, R. *et al.* External mechanical cues trigger the establishment of the anterior-posterior axis in early mouse embryos. *Developmental Cell* 27, 131–144 (2013).

[92] Yeung, T. *et al.* Effects of substrate stiffness on cell morphology, cytoskeletal structure, and adhesion. *Cell Motility and the Cytoskeleton* 60, 24–34 (2005).

[93] Pelham, R.J. & Wang, Y.l. Cell locomotion and focal adhesions are regulated by substrate flexibility. *Proceedings of the National Academy of Sciences* 94, 13661–13665 (1997).

[94] Plotnikov, S.V. & Waterman, C.M. Guiding cell migration by tugging. *Current Opinion in Cell Biology* 25, 619–626 (2013).

[95] Lo, C.M., Wang, H.B., Dembo, M., & Wang, Y.l. Cell movement is guided by the rigidity of the substrate. *Biophysical Journal* 79, 144–152 (2000).

[96] Kim, S.N. *et al.* ECM stiffness regulates glial migration in Drosophila and mammalian glioma models. *Development* 141, 3233–3242 (2014).

[97] Giannone, G. & Sheetz, M.P. Substrate rigidity and force define form through tyrosine phosphatase and kinase pathways. *Trends in Cell Biology* 16, 213–223 (2006).

[98] Swift, J. *et al.* Nuclear lamin-A scales with tissue stiffness and enhances matrix-directed differentiation. *Science* 341, 1240104 (2013).

[99] Buxboim, A. *et al.* Matrix elasticity regulates lamin-a,c phosphorylation and turnover with feedback to actomyosin. *Current Biology* 24, 1909–1917 (2014).

[100] Raab, M. *et al.* Crawling from soft to stiff matrix polarizes the cytoskeleton and phosphoregulates myosin-II heavy chain. *The Journal of Cell Biology* 199, 669–683 (2012).

[101] Gomez, T.M., Robles, E., Poo, M.m., & Spitzer, N.C. Filopodial calcium transients promote substrate-dependent growth cone turning. *Science* 291, 1983–1987 (2001).

[102] Franze, K. The mechanical control of nervous system. *Development* 140, 3069–3077 (2013).

[103] Tyler, W.J. The mechanobiology of brain function. *Nature Reviews Neuroscience* 13, 867–878 (2012).

[104] Harland, B., Walcott, S., & Sun, S.X. Adhesion dynamics and durotaxis in migrating cells. *Physical Biology* 8, 015011 (2011).

[105] Haeger, A., Wolf, K., Zegers, M.M., & Friedl, P. Collective cell migration: guidance principles and hierarchies. *Trends in Cell Biology* (2015).

[106] Singh, S.P., Schwartz, M.P., Lee, J.Y., Fairbanks, B.D., & Anseth, K.S. A peptide functionalized poly(ethylene glycol) (PEG) hydrogel for investigating the influence of biochemical and biophysical matrix properties on tumor cell migration. *Biomaterials Science* 2, 1024–1034 (2014).

[107] Chao, P.h.G., Sheng, S.C., & Chang, W.R. Micro-composite substrates for the study of cell-matrix mechanical interactions. *Journal of the Mechanical Behavior of Biomedical Materials* 38, 232–241 (2014).

[108] Martinez, J.S., Lehaf, A.M., Schlenoff, J.B., & Keller, T.C.S. Cell durotaxis on polyelectrolyte multilayers with photogenerated gradients of modulus. *Biomacromolecules* 14, 1311–1320 (2013).

[109] Nemir, S., Hayenga, H.N., & West, J.L. PEGDA hydrogels with patterned elasticity: Novel tools for the study of cell response to substrate rigidity. *Biotechnology and Bioengineering* 105, 636–644 (2010).

[110] Wong, S., Guo, W.h., Hoffecker, I., & Wang, Y.l. Preparation of a micropatterned rigid-soft composite substrate for probing cellular rigidity sensing. *Methods in Cell Biology* 121, 3–15 (2014).

[111] Wong, S., Guo, W.H., & Wang, Y.L. Fibroblasts probe substrate rigidity with filopodia extensions before occupying an area. *Proceedings of the National Academy of Sciences of the United States of America* 111, 17176–17181 (2014).

[112] Orsi, G., Fagnano, M., De Maria, C., Montemurro, F., & Vozzi, G. A new 3d concentration gradient maker and its application in building hydrogels with a 3d stiffness gradient. *Journal of Tissue Engineering and Regenerative Medicine* (2014).

[113] Engler, A.J. *et al.* Myotubes differentiate optimally on substrates with tissue-like stiffness: pathological implications for soft or stiff microenvironments. *The Journal of Cell Biology* 166, 877–887 (2004).

[114] Richert, L., Engler, A.J., Discher, D.E., & Picart, C. Elasticity of native and cross-linked polyelectrolyte multilayer films. *Biomacromolecules* 5, 1908–1916 (2004).

[115] Lange, J.R. & Fabry, B. Cell and tissue mechanics in cell migration. *Experimental Cell Research* 319, 2418–2423 (2013).

[116] Willits, R.K. & Skornia, S.L. Effect of collagen gel stiffness on neurite extension. *Journal of Biomaterials Science, Polymer Edition* 15, 1521–1531 (2004).

[117] Gefen, A. & Margulies, S.S. Are in vivo and in situ brain tissues mechanically similar? *Journal of Biomechanics* 37, 1339–1352 (2004).

[118] Koch, D., Rosoff, W.J., Jiang, J., Geller, H.M., & Urbach, J.S. Strength in the periphery: growth cone biomechanics and substrate rigidity response in peripheral and central nervous system neurons. *Biophysical Journal* 102, 452–460 (2012).

[119] Kolahi, K.S. *et al.* Effect of substrate stiffness on early mouse embryo development. *PLoS ONE* 7, e41717 (2012).

[120] Cheng, C.M., LeDuc, P.R., & Lin, Y.W. Localized bimodal response of neurite extensions and structural proteins in dorsal-root ganglion neurons with controlled polydimethylsiloxane substrate stiffness. *Journal of Biomechanics* 44, 856–862 (2011).

[121] Kerstein, P.C. *et al.* Mechanosensitive TRPC1 channels promote calpain proteolysis of talin to regulate spinal axon outgrowth. *The Journal of Neuroscience* 33, 273–285 (2013).

[122] Tai, G., Reid, B., Cao, L., & Zhao, M. Electrotaxis and wound healing: experimental methods to study electric fields as a directional signal for cell migration. *Methods in Molecular Biology* 571, 77–97 (2009).

[123] Cortese, B., Palamà, I.E., D'Amone, S., & Gigli, G. Influence of electrotaxis on cell behaviour. *Integrative Biology: Quantitative Biosciences from Nano to Macro* 6, 817–830 (2014).

[124] Ahirwar, D.K. *et al.* Non-contact method for directing electrotaxis. *Scientific Reports* 5, 11005 (2015).

[125] Charest, J.L., Eliason, M.T., García, A.J., & King, W.P. Combined microscale mechanical topography and chemical patterns on polymer cell culture substrates. *Biomaterials* 27, 2487–2494 (2006).

[126] Kundu, A. *et al.* Superimposed topographic and chemical cues synergistically guide neurite outgrowth. *Lab on a Chip* 13, 3070–3081 (2013).

[127] Spedden, E., Wiens, M.R., Demirel, M.C., & Staii, C. Effects of surface asymmetry on neuronal growth. *PLoS ONE* 9, e106709 (2014).

[128] Lee, C.y. *et al.* Actin depolymerization under force is governed by lysine 113:glutamic acid 195-mediated catch-slip bonds. *Proceedings of the National Academy of Sciences* 110, 5022–5027 (2013).

[129] Riahi, R. *et al.* Notch1–Dll4 signalling and mechanical force regulate leader cell formation during collective cell migration. *Nature Communications* 6, 6556 (2015).

[130] Wymer, C.L., Wymer, S.A., Cosgrove, D.J., & Cyr, R.J. Plant cell growth responds to external forces and the response requires intact microtubules. *Plant Physiology* 110, 425–430 (1996).

[131] Magdesian, M.H. *et al.* Rapid mechanically controlled rewiring of neuronal circuits. *The Journal of Neuroscience* 36, 979–987 (2016).

[132] Ehrlicher, A. *et al.* Guiding neuronal growth with light. *Proceedings of the National Academy of Sciences* 99, 16024–16028 (2002).

[133] Ehrlicher, A. *et al.* Optical neuronal guidance. *Methods in Cell Biology* 83, 495–520 (2007).

[134] Sun, Y., Jallerat, Q., Szymanski, J.M., & Feinberg, A.W. Conformal nanopatterning of extracellular matrix proteins onto topographically complex surfaces. *Nature Methods* (2014).

[135] Jannat, R.A., Dembo, M., & Hammer, D.A. Neutrophil adhesion and chemotaxis depend on substrate mechanics. *Journal of physics. Condensed matter : an Institute of Physics journal* 22, 194117 (2010).

[136] Croze, O.A., Ferguson, G.P., Cates, M.E., & Poon, W.C. Migration of chemotactic bacteria in soft agar: role of gel concentration. *Biophysical Journal* 101, 525–534 (2011).

[137] Leoni, M. & Sens, P. Polarization of cells and soft objects driven by mechanical interactions: Consequences for migration and chemotaxis. *Physical Review E* 91, 022720 (2015).

[138] Tseng, P., Pushkarsky, I., & Di Carlo, D. Metallization and biopatterning on ultra-flexible substrates via dextran sacrificial layers. *PLoS ONE* 9, e106091 (2014).

[139] Castaño, A.G. *et al.* Protein patterning on hydrogels by direct microcontact printing: application to cardiac differentiation. *RSC Advances* 4, 29120–29123 (2014).

[140] Drescher, U., Bonhoeffer, F., & Müller, B.K. The Eph family in retinal axon guidance. *Current Opinion in Neurobiology* 7, 75–80 (1997).

[141] Goodman, S.L., Risse, G., & von der Mark, K. The E8 subfragment of laminin promotes locomotion of myoblasts over extracellular matrix. *The Journal of Cell Biology* 109, 799–809 (1989).

[142] Mehlen, P. & Furne, C. Netrin-1: when a neuronal guidance cue turns out to be a regulator of tumorigenesis. *Cellular and molecular life sciences: CMLS* 62, 2599–2616 (2005).

[143] Mills, K.L., Zhu, X., Takayama, S., & Thouless, M.D. The mechanical properties of a surface-modified layer on poly(dimethylsiloxane). *Journal of materials research* 23, 37–48 (2008).

[144] van Dommelen, J.a.W., van der Sande, T.P.J., Hrapko, M., & Peters, G.W.M. Mechanical properties of brain tissue by indentation: interregional variation. *Journal of the Mechanical Behavior of Biomedical Materials* 3, 158–166 (2010).

[145] Levental, I., Georges, P.C., & Janmey, P.A. Soft biological materials and their impact on cell function. *Soft Matter* 3, 299–306 (2007).

[146] Serafini, T. *et al.* The netrins define a family of axon outgrowth-promoting proteins homologous to C. elegans UNC-6. *Cell* 78, 409–424 (1994).

[147] Shirasaki, R., Mirzayan, C., Tessier-Lavigne, M., & Murakami, F. Guidance of circumferentially growing axons by netrin-dependent and -independent floor plate chemotropism in the vertebrate brain. *Neuron* 17, 1079–1088 (1996).

[148] Mills, K.L., Zhu, X., Lee, D., Takayama, S., & Thouless, M.D. Properties of the surface-modified layer of plasma-oxidized poly(dimethylsiloxane). In *Symposium Z – Mechanics of Nanoscale Materials and Devices*, volume 924 of *MRS Online Proceedings Library Archive* (2006).

[149] Chan, E.P. & Crosby, A.J. Spontaneous formation of stable aligned wrinkling patterns. *Soft Matter* 2, 324–328 (2006).

[150] Kim, B.C. *et al.* Guided fracture of films on soft substrates to create micro/nano-feature arrays with controlled periodicity. *Scientific Reports* 3 (2013).

[151] Huck, W.T.S. *et al.* Ordering of spontaneously formed buckles on planar surfaces. *Langmuir* 16, 3497–3501 (2000).

[152] Bowden, N., Brittain, S., Evans, A.G., Hutchinson, J.W., & Whitesides, G.M. Spontaneous formation of ordered structures in thin films of metals supported on an elastomeric polymer. *Nature* 393, 146–149 (1998).

[153] Wu, M.H. Simple poly(dimethylsiloxane) surface modification to control cell adhesion. *Surface and Interface Analysis* 41, 11–16 (2009).

[154] Wang, L., Sun, B., Ziemer, K.S., Barabino, G.A., & Carrier, R.L. Chemical and physical modifications to poly(dimethylsiloxane) surfaces affect adhesion of Caco-2 cells. *Journal of Biomedical Materials Research. Part A* 93, 1260–1271 (2010).

[155] Schwarz, U.S. & Soiné, J.R.D. Traction force microscopy on soft elastic substrates: A guide to recent computational advances. *Biochimica et Biophysica Acta (BBA) - Molecular Cell Research* 1853, 3095–3104 (2015).

[156] Umedachi, T., Vikas, V., & Trimmer, B.A. Softworms : the design and control of non-pneumatic, 3d-printed, deformable robots. *Bioinspiration & Biomimetics* 11, 025001 (2016).

[157] Serafini, T. *et al.* Netrin-1 Is Required for Commissural Axon Guidance in the Developing Vertebrate Nervous System. *Cell* 87, 1001–1014 (1996).

[158] Ganiko, L., Martins, A.R., Espreáfico, E.M., & Roque-Barreira, M.C. Neutrophil haptotaxis induced by the lectin KM+. *Glycoconjugate Journal* 15, 527–530 (1998).

[159] de Toledo, K.A., Bernardes, E.S., Baruffi, M.D., & Roque-Barreira, M.C. Neutrophil haptotaxis induced by mouse MNCF: interactions with extracellular matrix glycoproteins probably contribute to overcoming the anti-inflammatory action of dexamethasone. *Inflammation Research: Official Journal of the European Histamine Research Society ... [et Al.]* 56, 368–376 (2007).

[160] Thomas, G., Burnham, N.A., Camesano, T.A., & Wen, Q. Measuring the Mechanical Properties of Living Cells Using Atomic Force Microscopy. *Journal of Visualized Experiments* (2013).